Green-Synthesized Nano-Hydroxyapatite using *Terminalia arjuna* enhancing Osteogenesis in MG-63 Cells: A Promising Approach for Bone Regeneration

Suba Sri M. and Usha R.*
Department of Microbiology, Karpagam Academy of Higher Education, Coimbatore, Tamil Nadu, INDIA
*usha.anbu09@gmail.com

Abstract

Hydroxyapatite (HA) is a biologically unique extremely bioactive, osteoconductive and biodegradable calcium phosphate which is chemically and structurally similar to the mineral phase of natural bone. It is the material of choice for bone regeneration and tissue engineering applications. In the current work nano-hydroxyapatite (nHA) was synthesized by eco-friendly co-precipitation method using Terminalia arjuna bark extract known for its rich phytochemical profile, medicinal properties, reducing and stabilizing potential. The developed nHA materials were then characterized using a number of physicochemical techniques such as UV-Visible spectroscopy in which surface plasmon resonance was observed, X-ray diffraction was performed to calculate the crystallite size, Fourier Transform Infrared Spectroscopy was done to identify the major important functional groups. Particle size distribution analysis reveals the uniform distribution of nanoparticles in the size range from 50 to 100 nm. The antimicrobial activity of the developed nano particle was tested against both Gram-positive and Gram-negative bacterial strains showing strong anti-bacterial property. Besides, the nHA was electrospun into a nanofibrous scaffold through electrospinning which resembles the extracellular matrix (ECM) of native bone tissue. The developed scaffold was then subjected to mechanical characterization to ensure accuracy in stress/strain analysis and biocompatibility by simulated body fluid study. In vitro cytotoxicity testing was done to determine the toxicity of the developed scaffold. Cell viability of 77.16 % in 25 µg/mL sample concentration was observed against chemically induced bone loss. The early osteogenesis process was determined by alkaline phosphatase (ALP) activity in which the highest ALP production was observed as 5.123 ng/ml and late osteogenesis was evaluated by calcium mineralization assay by alizarin red S staining. The results showed that the synthesized nHA from T. arjuna bark extract exhibits osteoprotective effects with increased osteogenic differentiation of MG-63 cells. The results demonstrate the therapeutic potential of Terminalia arjuna mediated nano-hydroxyapatite as a next-generation bioceramic material with potential uses in bone grafts, orthopedic implants and scaffolds for tissue engineering.

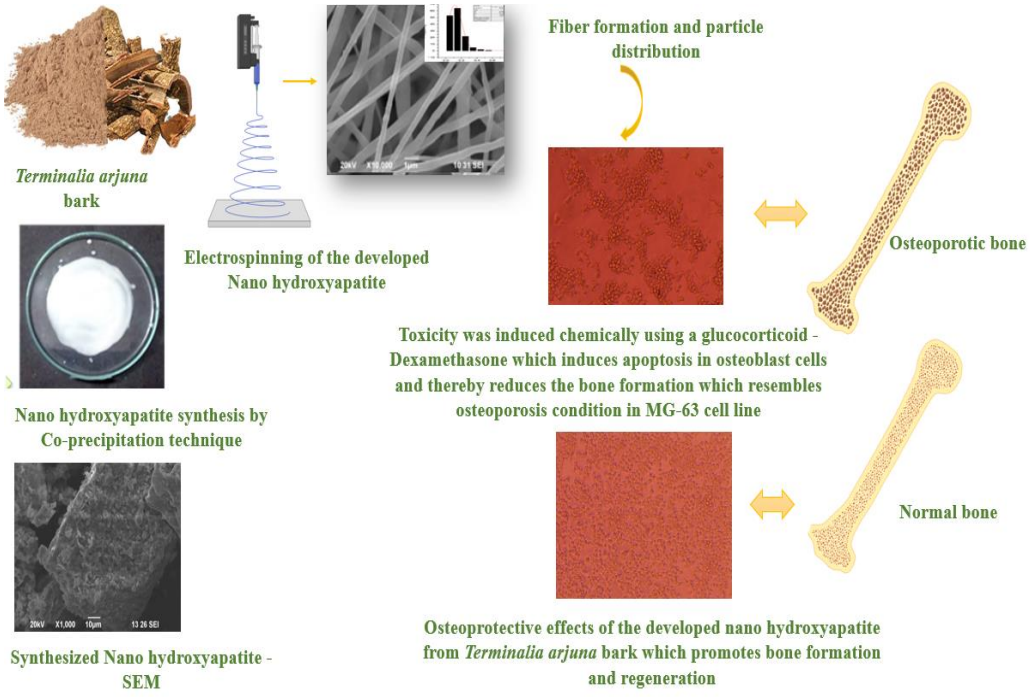

Graphical Abstract

https://doi.org/10.25303/2011rjbt1540173

Keywords: *Terminalia arjuna* nano hydroxyapatite, UV-Visible spectrophotometer, XRD, FTIR, SEM, Electrospun scaffold, MG-63, *in vitro* cytotoxicity, osteoprotective effect, human specific alkaline phosphatase, Alizarin red S Stain.

Introduction

Nanotechnology takes a different approach to overcome the shortcomings of bulk materials, which have been the focus of recent biomaterial research. Nanocrystalline hydroxyapatite (nHA) is a ceramic biomaterial with osteoconductive, bioactivity and biocompatibility. Calcium phosphate occurs naturally as hydroxyapatite, a mineral that is found in teeth and bones. Even while bones cannot regrow naturally, it has been shown that nHA can be artificially generated utilising a variety of polymers[32]. The crystal structure of hydroxyapatite is primarily hexagonal, with two different types of Ca sites. The first site has nine oxygen atoms and forms a polyhedron, whereas the second site has five oxygen atoms and one hydroxyl group[13].

The creation of biomaterials comprising of hydroxyapatite and antibiotics is a highly successful method in bone tissue engineering for restoring bone loss. Because of their special qualities, hydroxyapatite nanoparticles made via biological means have several benefits and have drawn a lot of attention. To make hydroxyapatite nanoparticles, an aqueous solution of calcium and phosphate salt was used in co-precipitation technique. One disadvantage of co-precipitation in aqueous solution is the agglomeration of particles in hydroxyapatite. Instead of using an aqueous solution as a templating agent, plant extracts have been created to prevent the hydroxyapatite nanoparticles from aggregating[11].

Since ancient times, natural products have dominated human pharmacopoeia and are acknowledged as an infinite source of medicine[27]. They are more effective with fewer side effects and are less expensive[28]. The application of plant and its material in healthcare is widespread in both developed and developing nations which includes the usage of botanical medicines (either by themselves or in conjunction with prescription medications). Natural products continue to have an impact on the development of new drugs and orthopaedics has seen a surge in interest in recent years. *Terminalia arjuna* (TA) is a deciduous tree that belongs to the family Combretaceae and is found all over India. Its numerous therapeutic benefits are widely acknowledged in Ayurveda or Indian traditional medicine[15].

Bone fractures in both humans and animals can be effectively treated with TA bark paste. The use of bark pastes and plastering with the actual bark is thought to accelerate the regeneration of fractured bones. Indeed, the barks decoction is used medicinally to reduce inflammation and pain[35]. Traumatic incidents or bone damage cause significant bone loss resulting in size abnormalities and the need for bone substitutes to aid in regeneration. Calcium phosphate ceramics have become an unavoidable material for bone substitutes in recent decades. Along with biodegradability and biocompatibility, bioactivity is its most important component[34]. *T. arjuna* has gained attention in biomedical research, particularly for its potential role in enhancing bone regeneration when integrated with bioceramic materials such as nano-hydroxyapatite. The present study used TA bark extracts for nano hydroxyapatite development, characterized and electrospunned into a nano fibrous scaffold. As a result, scaffolds were made with TA nano hydroxyapatite to promote the growth of new bone evaluated *in vitro* using MG-63 cell line.

Material and Methods

Collection and Extraction of *Terminalia arjuna* bark: *Terminalia arjuna* barks were collected from Coimbatore, Tamil Nadu, India. The collected bark was thoroughly washed with double distilled water and then dried. The dried barks were processed to make fine powder and stored. The extraction process was done by mixing bark powder with ethanol in the ratio of 1:10. Further Whatmann no. 1 filter paper was used to filter the solvent and the obtained filtrate was evaporated under vacuum drier. Finally brown residue was obtained and stored at -4ºC for further use[20].

Co-precipitation technique for the synthesis of nanohydroxyapatite using the bark extract of *Terminalia arjuna*: To the 5 ml of *Terminalia arjuna* bark extract, calcium chloride (0.55 g) was added and pH 10 was maintained using 0.8 M of sodium hydroxide. Likewise, disodium hydrogen phosphate (0.425 g) was added to the *Terminalia arjuna* bark extract and thoroughly mixed. Disodium hydrogen phosphate was added in drops to the churning mixture. As a result, gelatinous white precipitate was obtained. After one hour, the reaction mixture was left for 24 hours for aging. After obtaining the final precipitate, *Terminalia arjuna* hydroxyapatite nanoparticles were obtained in solution form and washed with distilled water until the pH reached neutral. To turn the resulting HAp precipitate into powder, it was dried for 12 hours at 60ºC in a hot air oven. Distilled water was also used to maintain control[30].

UV-Visible Spectrophotometer characterization of developed nanohydroxyapatite using the bark extract of *Terminalia arjuna*: Using UV-Vis spectroscopy, the produced nanohydroxyapatite from bark extract was investigated. The spectra were acquired in the 240–520 nm wavelength range by taking 1 cm^3 of both the control and bark extract samples using Eppendorf UV–Visible spectrophotometer. The maximum absorbance and plasmon peak of the control and plant extract-mediated nanohydroxyapatite were measured[37].

Fourier Transform Infra-red Spectroscopy characterization of developed nanohydroxyapatite using the bark extract of *Terminalia arjuna*: The produced hydroxyapatite nanoparticle from *T. arjuna* bark extracts was subjected to Fourier transform infrared spectroscopy

(FTIR) using a Shimadzu single reflection ATR accessory, over a spectrum ranges from 400–4000 cm^{-1} for the detection of chemical bonds and functional groups[1].

X-Ray diffraction characterization of developed nanohydroxyapatite using the bark extract of *Terminalia arjuna*: Produced hydroxyapatite nanoparticles from *T. arjuna* extract were subjected to X-Ray diffraction (XRD) patterns in the region of $0^{\circ} \leq 2\theta \leq 80^{\circ}$. After being developed using *T. arjuna* and a control in liquid form, the hydroxyapatite nanoparticles were subjected to centrifugation at 2500 RPM. Following a 30-to-40-minute drying process at 60˚C in a water bath, the pellet was ground into a fine powder for XRD assessment[10]. The lattice parameters of a developed *T. arjuna* nano hydroxyapatite and control were computed by the equation:

$$1/d2=4(h2+hk+k2)/3a2+l2/c2 \quad (1)$$

where 'd' denotes the distance across the atomic lattices in an interplanar plane and 'v' denotes the unit cell volume in hexagons formed by the *T. arjuna* nano hydroxyapatite and control by the equation:

$$V=\sqrt{3}/2*a\hat{}2*C \quad (2)$$

The crystallite size of the developed *T. arjuna* nano hydroxyapatite and control were calculated by the Debye-Scherrer equation from XRD pattern:

$$Dhkl=K\lambda/\beta 1/2 \cos \theta \quad (3)$$

where 'K' denotes the Debye-Scherrer constant, Dhkl is the crystallite size, 1/2 is the full width at half maximum (FWHM) of (111) peak (radian) and 'degrees' denote the diffraction angle.

Scanning Electron Microscope characterization of developed nanohydroxyapatite using the bark extract of *Terminalia arjuna*: The morphology of developed hydroxyapatite nanoparticle from *T. arjuna* bark extracts was determined by SEM at 20 kV. Micrographs were captured to observe the shape, surface texture and distribution of the nanoparticles[24].

Antimicrobial activity of developed nanohydroxyapatite using the bark extract of *Terminalia arjuna*: The generated hydroxyapatite nanoparticle was tested for its antibacterial susceptibility to pathogens such as *Escherichia coli, Staphylococcus aureus, Bacillus subtilis, Klebsiella pneumoniae, Proteus mirabilis* and *Pseudomonas aeruginosa*.

The test organisms were swabbed onto the prepared nutrient agar plates. On the swabbed plate, wells were created and loaded with the standard streptomycin, solvent and the produced hydroxyapatite nanoparticle (plant extract and control). Following incubation at 37˚C/24 hours, zone of inhibition was noted[4].

Electrospinning of developed nanohydroxyapatite using the bark extract of *Terminalia arjuna*: 4:2 of the developed nanohydroxyapatite from *Terminalia arjuna* bark and poly-β-hydroxy butyrate were mixed with 7:3 of chloroform and dimethyl formamide. Then it was stirred at 35˚C for 3 hours in the magnetic stirrer. The completely dissolved mixture was subjected to electrospinning by using a syringe (10 ml) with blunt needle made of stainless steel (0.7 mm diameter). 12 kV high voltage was supplied with a flow rate 2500 µl/hr. Finally using the aluminium foil sheet fibers were collected with 8 cm distance from the needle tip. Then the fibers were deposited and formed as a nanofibrous scaffold mat within 4 hours[14].

Mechanical characterization of developed *T. arjuna* nanofibrous scaffold

Thickness (ASTM D 1777-96): The thickness gage Tilmet (ASTM D 1777-96) was used to determine the thickness of the developed the nanofibrous scaffold.

Tensile Strength (Zwick/Roell): The ZwickRoell testing machine was used to determine the nanofibrous scaffold's characteristics at a 5 mm/min cross head speed. Scaffolds of length 10 cm and breadth 2 cm were collected for analysis in order to find the average breaking strength and elongation.

Wetting ability by Water contact angle: Drop shape analysis was performed to determine the wettability of the developed nanofibrous scaffold. The surface was sprayed with 20µl of double distilled water at room temperature to measure the contact angle which indicates the wetting ability of the scaffold[40].

Fourier Transform Infra-red Spectroscopy analysis of the developed nanofibrous scaffold: Using *Terminalia arjuna* hydroxyapatite nanoparticle and poly-ß-hydroxy butyrate, a nanofibrous scaffold was created. Its chemical structure and functional bonds were examined by Fourier transform infrared spectrometer[39] (Shimadzu-single reflection ATR accessory) with the spectrum ranges from 400-4000 cm^{-1}.

Scanning Electron Microscopy analysis of the developed nanofibrous scaffold: The topology of the nanofibrous scaffold from *Terminalia arjuna* nano hydroxyapatite with PHB was analyzed using SEM. Diameters of the individual nanofibers and particles were measured using image J software. The obtained data were analyzed using Origin Pro software. The results were presented as mean particle size ± standard deviation with size distribution graph[36].

Bioactivity of developed nanofibrous scaffold: The formation of apatite-like structure after immersion in simulated body fluid (SBF) confirms the bioactivity of the scaffold. The bioactivity test is necessary and preliminary test of implanting the scaffold inside the human bone. The developed nanofibrous scaffolds were cut into 3*3 cm and immersed in a 14 ml of SBF solution with pH 7.4 and

incubated at 37˚C for 7 days. The simulated body fluid solution was prepared according to the Kokubo's protocol. The morphology of the immersed scaffold was visualized after incubation period under the Scanning electron microscope[19].

***In vitro* cytotoxicity determination of the developed *Terminalia arjuna* nano fibrous scaffold:** *In vitro* cytotoxicity of the developed *Terminalia arjuna* nano hydroxyapatite was determined by MTT assay. MG-63 (Osteosarcoma cells) was procured from NCCS, Pune, India maintained in Dulbecco's modified Eagles medium (DMEM). 2 days old cells were trypsinized and suspended in 10% growth medium. $5x10^3$ cells/well was seeded in 96 well plate and kept for incubation at 37ºC in humidified 5% CO_2 incubator. 1 mg of the developed nano composite from *T. arjuna* was weighed and dissolved in 1mL DMEM using a cyclomixer. The sample solution was filtered through 0.22 µm Millipore syringe filter to ensure the sterility. After attaining sufficient growth in 96 well plate, the prepared compounds were added at different concentrations (100 µg/ml, 50 µg/ml, 25 µg/ml, 12.5 µg/ml and 6.25 µg/ml) and were added to the respective wells and incubated at 37°C in a humidified 5% CO2 incubator.

Untreated cells were kept as control. The cytotoxicity was determined by direct microscopic observation in phase contrast microscope and by MTT assay. After incubation period, the samples added in the wells were removed and mixed with 30µl of reconstituted MTT solution (15 mg of MTT in 3 ml PBS filter sterilized) and incubated at 37ºC/4 hours in a humidified 5% CO_2 incubator. Further cells were centrifuged and the supernatant was taken and mixed with 100µl of MTT solubilization solution which solubilizes the formazan crystals. Using microplate reader, the absorbances were recorded at 540 nm[7].

The percentage of viability was calculated by using the formula:

$$\% \text{ of viability} = \frac{\text{Mean OD Samples x 100}}{\text{Mean OD of control group}}$$

Osteoprotective effects of the developed *Terminalia arjuna* nano fibrous scaffold: Osteoprotective effects of the developed nano hydroxyapatite were done to determine its potential as a bone-regenerative therapeutic agent against chemically induced bone loss. Dexamethasone is a glucocorticoid which induces apoptosis in osteoblast cells and thereby reduces the bone formation which resembles osteoporosis condition. Determining the osteoprotective effect with the developed nano composite confirms whether the osteoblast cells are viable and have ability to proliferate and differentiate in presence of dexamethasone. This study demonstrates the developed nano composite capacity to protect bone forming cells under stress. Similar to *in vitro* cytotoxicity analysis protocol, after attaining sufficient growth, dexamethasone(5µM) was added to induce toxicity and incubated for one hour and freshly prepared samples (developed nano composite from *T. arjuna*) were added at concentrations of 25µg/ml, 12.5 µg/ml, 6.25 µg/ml, 3.1 µg/ml and 1.5 µg/ml respectively. Each concentration was added in triplicate to the respective wells and incubated at 37°C in a humidified 5% CO_2 incubator. Untreated control cells and dexamethasone alone treated wells were also maintained. The viability of cells was evaluated by direct observation of cells by inverted phase contrast microscope and followed by MTT assay method[29].

Human specific alkaline phosphatase activity of the developed *Terminalia arjuna* nano composite by Sandwich ELISA: Alkaline phosphatase (ALP) is a key marker of early osteogenesis. The protective and restorative effects on osteoblast cells by the developed nano composite was determined by the following method. After attaining sufficient growth of MG-63 cell line, dexamethasone(5µM) and sample 25µg/ml (developed nano composite from *T. arjuna*) were added in 4 wells and incubated at 37°C in order to determine whether the samples could counter the effects of dexamethasone. Alkaline phosphatase activity was determined by sandwich ELISA in which the cells were precoated with anti-ALP antibody. Blank, standard and sample 100 µl each were added to the respective wells, were sealed and incubated at 37ºC/90 minutes. Using wash buffer the plates were unsealed and washed for 5 times.

The biotinylated antibody solution (100 µl) was added to all the wells, sealed and again incubated at 37 ˚C/1 hour. The biotin conjugated anti-ALP antibody was used in detecting antibodies which binds to the different site of ALP protein. After incubation, the wells were washed with wash buffer followed by the addition of streptavidin – HRP conjugate-solution (100 µl) and incubated at 37˚C/ 30 minutes. HRP (Horseradish peroxidase)- Streptavidin will bind to biotin forming the complete "sandwich complex". After incubation plates were washed with wash buffer.

TMB substrate solution (90 µl) was added to each well and kept for incubation at 37˚C/15 minutes in dark. HRP enzyme converts TMB (3,3',5,5'- Tetramethylbenzidine) substrate into blue color. After incubation period stop solution (50 µl) was added to all the wells which leads the colour change from blue to yellow. Finally, OD was measured at 450 nm in a microplate reader. The density of yellow color is proportional to the presence of ALP amount of the sample[25].

Calcium release assay of the developed *Terminalia arjuna* nano composite by Alizarin Red S staining: Calcium release assay by Alizarin Red S (ARS) staining was done for the developed nano composite in order to evaluate the mineralization potential of the developed nano composite under dexamethasone induced toxicity. *In vitro* quantification of ARS staining was done spectrophotometrically by the following method. After attaining sufficient growth of MG-63 cell line, dexamethasone(5µM) and 25µg/ml *Terminalia arjuna* nano

composite were added in four wells and incubated at 37°C in a humidified 5% CO_2 incubator. ARS was done for day 1, 7, 14 and 28. Tissue culture plates were washed with PBS buffer for three times.

The cells were fixed with 2.5% glutaraldehyde for 15 minutes. Then the cells were washed with distilled water for three times. Water was drained completely and alizarin red S stain was added (14mg/mL; pH 4.1) and kept for 30 minutes. Dye was removed by washing the plates with distilled water for five times. After washing, the plates were kept at -20^{0}C/5 minutes in tilted position. Further 200µL of acetic acid (10%) was added and kept for 30 minutes and vortexed. Finally, the tubes were heated at 85^{0}C/10 minutes and subjected to ice for 5 minutes. The supernatant was taken after centrifugation at 10,000 rpm, the OD was measured at 405nm and morphological images were taken in the phase contrast microscope[21].

Statistical Analysis: The experiments were done in triplicate and results represented as mean ± standard deviation. One-way ANOVA and Dunnets test were performed to analyse data. The value of $p < 0.001$ indicates statistically significant difference in the sample compared to control groups.

Results and Discussion

Co-precipitation technique for the synthesis of nanohydroxyapatite using the bark extract of *Terminalia arjuna*: Utilizing the precursors (calcium chloride and disodium hydrogen phosphate) added for the co-precipitation method to synthesize nanohydroxyapatite and using the bark extract of *Terminalia arjuna* as a templating agent, a white precipitate was produced following a 24-hour stirring period. After 12 hours air dried powder was obtained. Similarly, hydroxyapatite nanoparticles utilized *Azadirachta indica* and *Coccinia grandis* as precursors, as well as di-sodium hydrogen phosphate and calcium chloride[24]. Hydroxyapatite nanoparticles in solution phase are synthesised using diammonium hydrogen phosphate and calcium nitrate tetrahydrate as precursors[8].

UV-Visible Spectrophotometer characterization of developed nanohydroxyapatite using the bark extract of *Terminalia arjuna*: The developed nanohydroxyapatite was characterized using a UV-visible spectrophotometer. The wavelength ranges from 200 to 700 nanometers, the spectrum was recorded. 2.349 is the maximum absorbance measured at a wavelength of 273 nm for control (figure 1a). Figure 1b depicts the UV-Visible measurement of nanohydroxyapatite synthesised using *Terminalia arjuna* bark extract, which has an absorbance of 0.947 at 286 nm. The surface Plasmon effect is caused by the synthesis of calcium apatite in plant extract and thus the highest absorbance was reached. Similarly, maximum absorbance was found at wavelengths of 278 nm and 272 nm in the UV-Visible spectrum of synthesized hydroxyapatite nanoparticles which contains folic acid and polyethylene glycol[22].

Fourier Transform Infra-red Spectroscopy characterization of developed nanohydroxyapatite using the bark extract of *Terminalia arjuna*: The biomolecules such as chemicals and functional groups present in the nano hydroxyapatite generated from *Terminalia arjuna* bark extract were represented by FTIR analysis. The existence of an acidic carbonate group is critical for hydroxyapatite nanoparticle characterisation because the human bone contains 4-6% carbonate weight[27]. The acidic carbonate and basic phosphate groups existence in the *Terminalia arjuna* nanohydroxyapatite are shown in table 1 and figure 2, indicating the synthesis of hydroxyapatite nanoparticles. The FTIR analysis of produced nanohydroxyapatite from bark extract of *Terminalia arjuna* and control is shown in table 1. The existence of carbonate, phosphate and alcohol confirms the formation of hydroxyapatite nanoparticle.

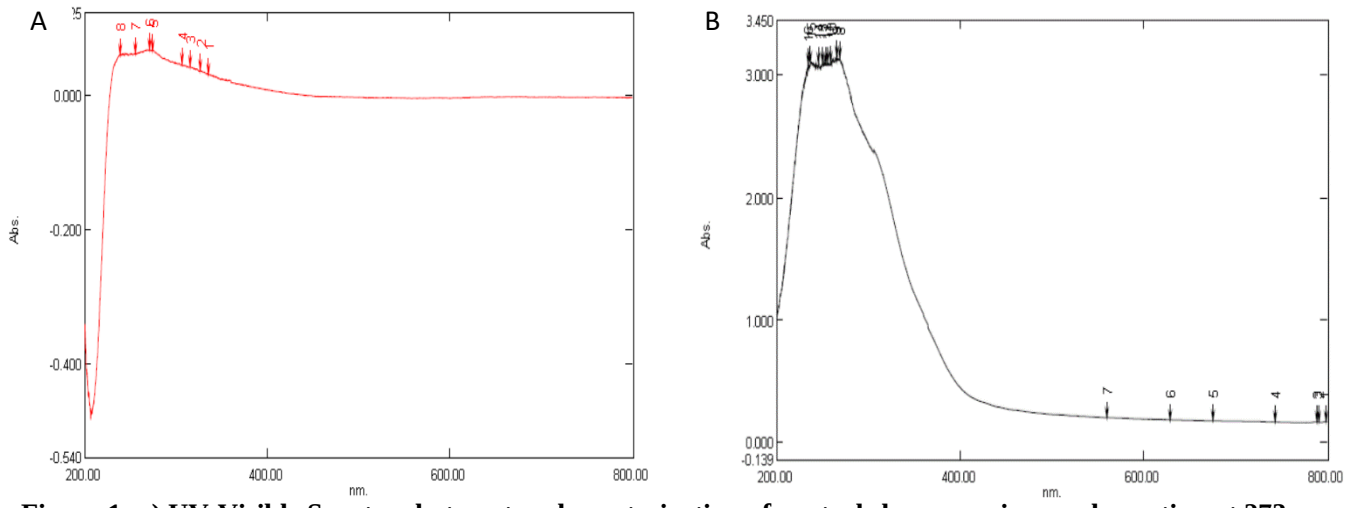

Figure 1: a) UV-Visible Spectrophotometer characterization of control shows maximum absorption at 273 nm. b) UV-Visible Spectrophotometer characterization of Terminalia arjuna nanohydroxyapatite shows maximum absorption at 286 nm

Figure 2a shows the FTIR examination of the developed control nano hydroxyapatite. The presence of OH functional group is shown by large and broad peaks at 3380.51 cm^{-1}. The carbonate and phosphate group existence were confirmed at 410.75 cm^{-1} and 1636.52 cm^{-1} for control. Figure 2b depicts the FTIR measurement of hydroxyapatite nanoparticles synthesised using *Terminalia arjuna* bark extract. A broad peak at 3483.02 cm^{-1} corresponds to alcohol group. Peaks at 1625.69 cm^{-1} correspond to carbonate group whereas 425.74 cm^{-1} validated the phosphate group.

The presence of an important functional group is indicated by the absorption band at 3571 cm^{-1} as alcohol while the carbonate groups in hydroxyapatite nanoparticle were primarily characterized by the peaks at 1458 cm^{-1}, 1412 cm^{-1} and 1456 cm^{-1} [3]. Comparably the vibrational modes of peak at 461 cm^{-1}, 566 cm^{-1}, 604 cm^{-1}, 962 cm^{-1}, 1034 cm^{-1} and 1100 cm^{-1} in the FTIR spectra of hydroxyapatite nanoparticles reveal the presence of phosphate group while peak at 3568 cm^{-1} corresponds to alcohol group existence[3].

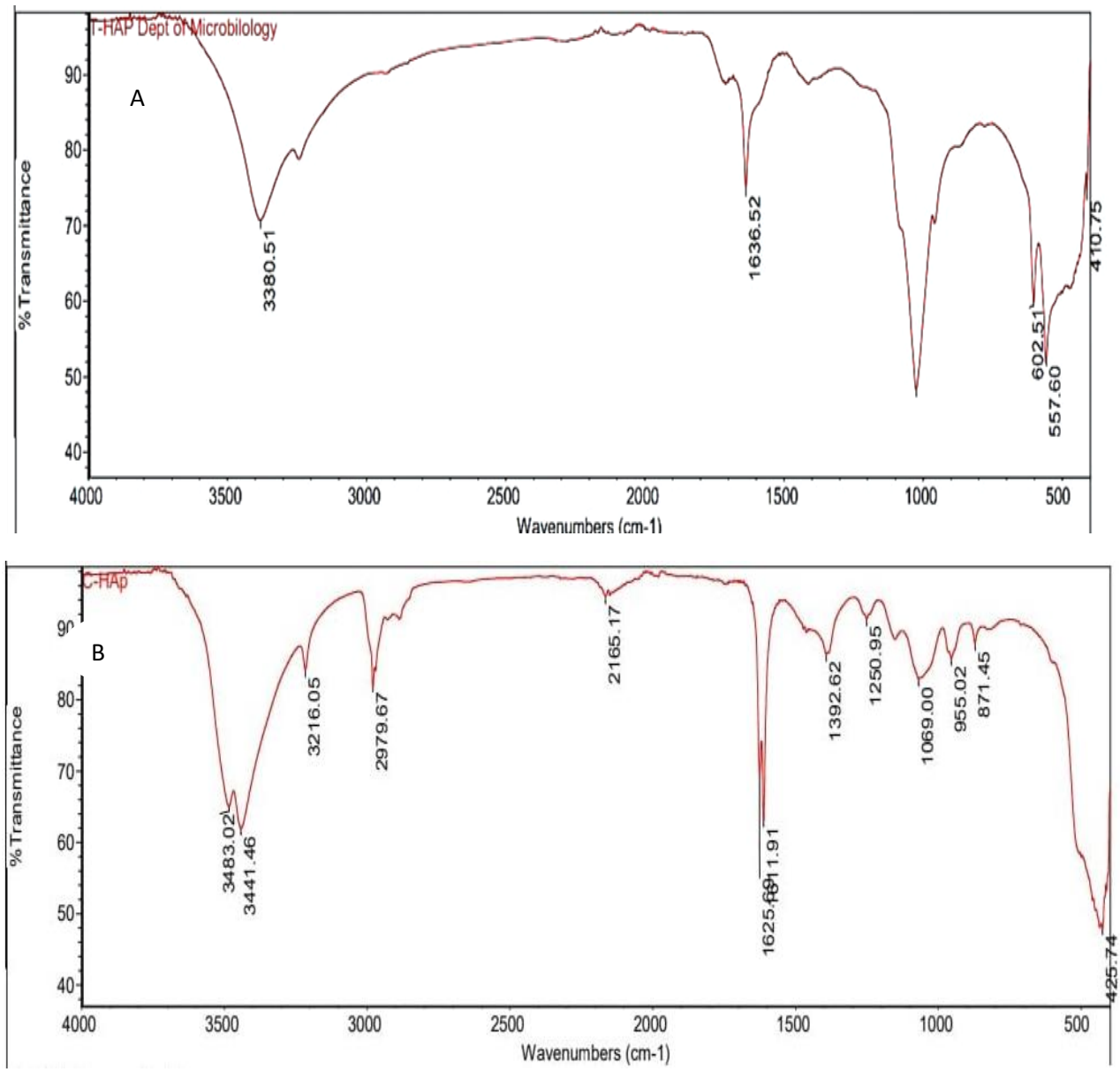

Figure 2: a) Control and b) Terminalia arjuna nanohydroxyapatite FTIR characterization shows the presence of important functional groups such as carbonate, phosphate and alcoholic group

Table 1
Fourier Transform Infra-red Spectroscopy characterization of the developed nanohydroxyapatite using the bark extract of *Terminalia arjuna* and control

S.N.	Control (cm^{-1})	Plant Extract (cm^{-1})	Functional groups
1	1636.52	1625.69	CO3 (Carbonate group)
2	410.75	425.74	PO4 (Phosphate group)
3	3380.51	3483.02	OH (Alcohol group)

X-Ray diffraction characterization of developed nanohydroxyapatite using the bark extract of *Terminalia arjuna*: The XRD technique is crucial for identifying the texture, crystallinity and residual stress for the developed nano hydroxyapatite. The morphology, crystallinity, heat stability and solubility of biomaterials can also alter, leading to modifications in their physical, chemical and biological characteristics. Inconsistent crystallinity may arise from lattice parameters being affected by minute variations pH and temperature during synthesis. Due to this, the most important method for determining crystallinity and lattice properties is the X-Ray diffraction study. Broad peaks in the 20º to 50º range suggest the existence of incomplete nanohydroxyapatite[23,41]. It was determined that the synthesized nanoparticles were pure hydroxyapatite with a hexagonal crystal structure compared with JCPDS (Joint Committee on Powder Diffraction Standards) data to the XRD patterns of generated nano hydroxyapatite using control and plant extracts.

A prominent peak in the 30-34 range can be seen in Miller's hydroxyapatite planes; this peak was created from control and extract from arjuna bark (111), (101) and (102). The formation of crystallite and crystalline composition determine the peak resolution. Table 2 shows the X-Ray diffraction study of the developed hydroxyapatite nanoparticles with lattice constant, unit cell volume and average crystallite size.

Figure 3a shows the XRD analysis of control nano hydroxyapatite, while figure 3b shows the XRD analysis of the developed nano hydroxyapatite utilizing *Terminalia arjuna* extract. The abrupt, high-intensity peaks at angles 25.9 and 31.8 corresponded to HAp crystals, with Miller indices (hkl values) of (002) and (211) respectively. XRD investigation revealed the hexagonal shape of the developed HAp crystals (PDF card numbers 009-0432 and 01-072-1243). According to the Scherrer formula, the formed HAp crystals were tiny crystallites that measured about 5 nm.

Table 2
X-Ray diffraction characterization of the developed nanohydroxyapatite using the bark extract of *Terminalia arjuna* and control

Sample	Peak (theta degree)	Lattice constant (Å) a=b	Lattice constant (Å) C	Unit Cell Volume V(Å^3)	Average Crystallite Size D
Control HAp	32	12.87	9.24	1325.43	25.62
Terminalia arjuna HAp	32	14.144	9.32	1614.69	31.13

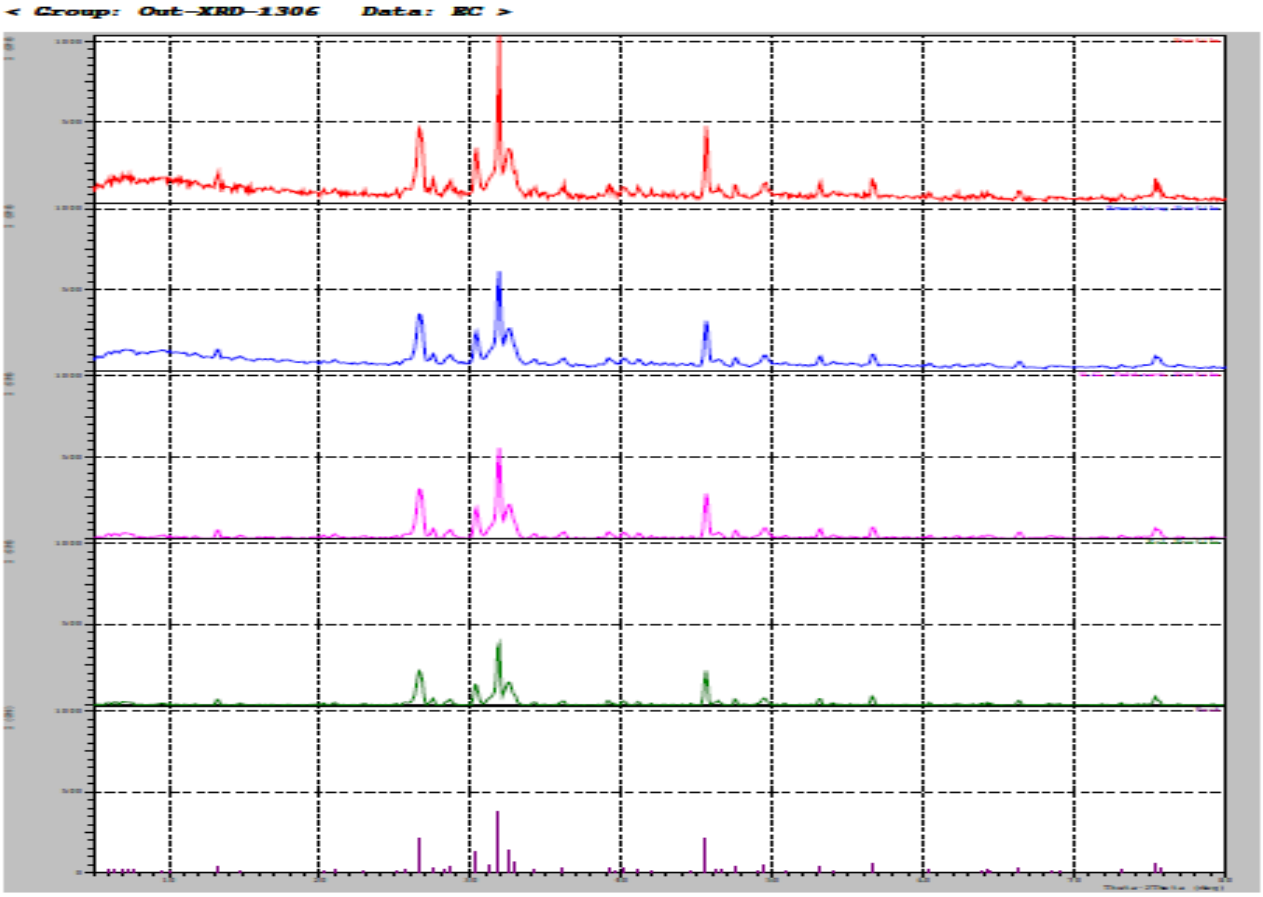

(A)

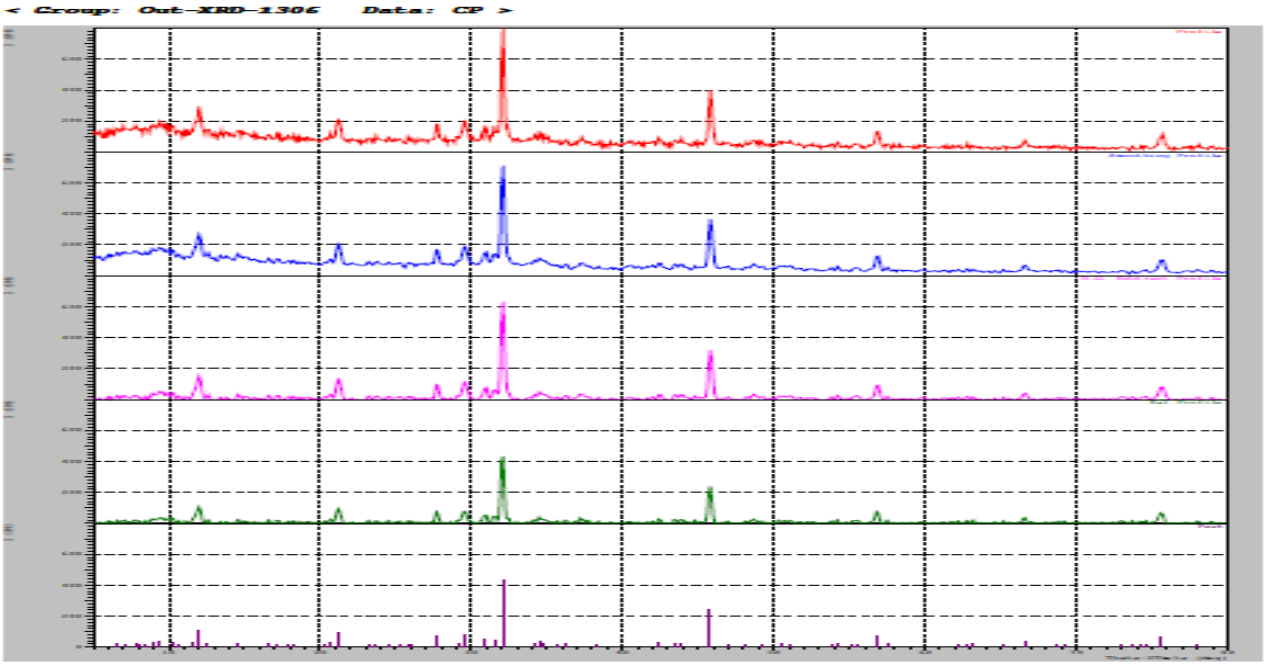

(B)

Figure 3: a) Control and b) Terminalia arjuna nanohydroxyapatite XRD characterization shows the most prominent peak at 32 degree which indicates the presence of hydroxyapatite according to JCPDS standard

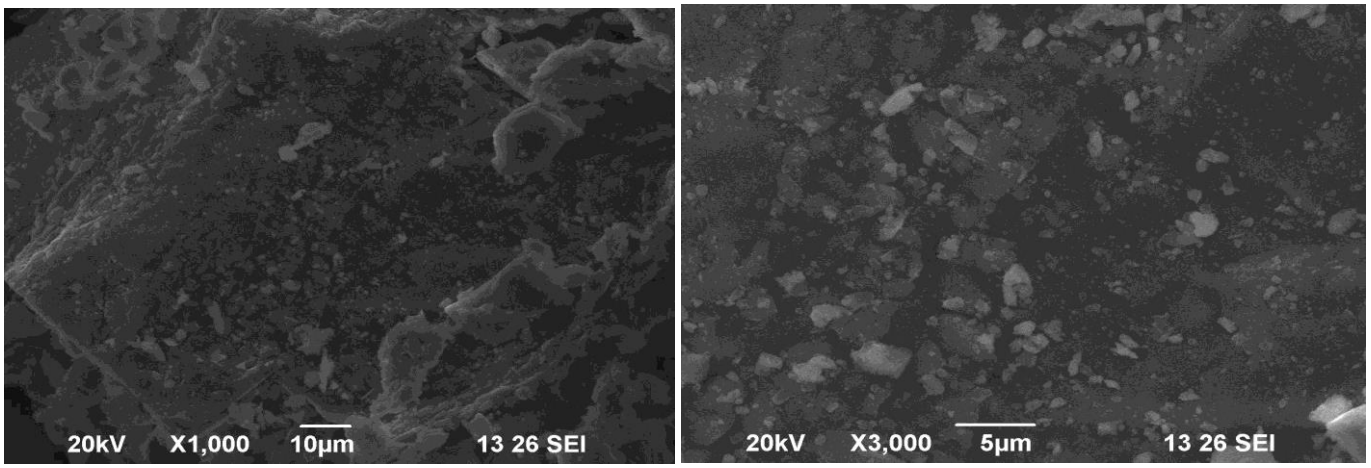

(A)

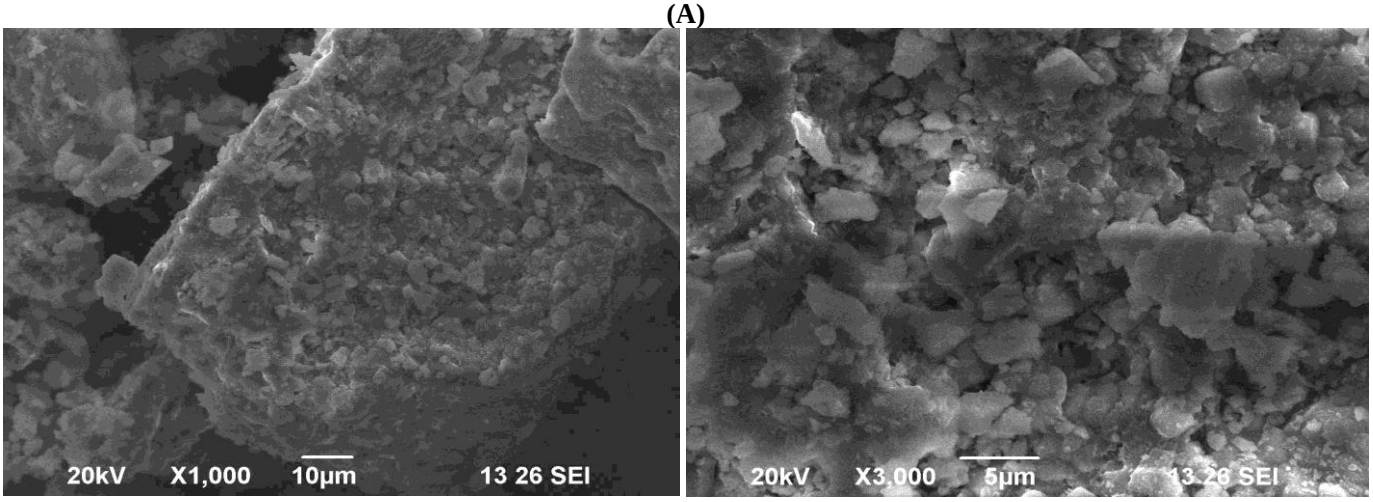

(B)

Figure 4: a) Control and b) Terminalia arjuna nanohydroxyapatite SEM characterization which shows poly crystalline morphology of the developed nanohydroxyapatite. The particle formation was found dense, aggregated, smooth and more in the *Terminalia arjuna* nanohydroxyapatite than

The diffraction peaks at 16.5 and 22.8 disappeared as the concentration of HAp increased. The lattice planes HAp (222) was linked to the 47.1 peak. The strong peak at 31.06, which forms narrow peaks in the diffractogram, signifies the nano hydroxyapatite's notable crystallinity[26].

Similarly, the commercial hydroxyapatite samples with Miller planes (002), (211), (300) and (310) were identical to the hydroxyapatite (HAp) powder standard data (JCPDS090432)[9].

Scanning Electron Microscope characterization of developed nanohydroxyapatite using the bark extract of *Terminalia arjuna*: The topology of the generated nano hydroxyapatite (SEM) was examined using a Scanning electron microscope. Rod-like hydroxyapatite Nps were investigated due to their resemblance to nano rod like structure present in human bone[2]. The hydroxyapatite nanoparticles created were aggregated, as indicated by SEM images at different magnifications such as 200X, 750X, 2000X and 5000X. The manufactured nano hydroxyapatite was examined in micrographs with sizes ranging from 2 to 100 m and a variety of shapes.

In SEM data showing crystal shape, the plant extract nanoparticle had the highest concentration of calcium apatite formation than the control.

In order to prevent agglomeration and facilitate the formation of nanohydroxyapatite, the plant extract can function as a powerful chelating, stabilizing and reducing agent. Figure 4a shows SEM images of control hydroxyapatite while Figure 4b shows SEM images of nanohydroxyapatite generated with *Terminalia arjuna* extract.

When the gel formed during the primary drying process, the hydroxyapatite samples agglomerated and took the form of nanorods[18]. Similarly, at 700°C temperature, the produced hydroxyapatite nanoparticle was found to be rod like needle shaped with a size of 82.63 nm[6].

Antimicrobial activity of developed nanohydroxyapatite using the bark extract of *Terminalia arjuna*: The developed hydroxyapatite's nano size provides a consistent contact with the surface area of the microbial cells, which results in a better interaction to inhibit the cell wall of micro-organisms. The antibacterial activities of the developed nanohydroxyapatite were determined using the qualitative method against *Escherichia coli, Staphylococcus aureus, Bacillus subtilis, Klebsiella pneumoniae, Proteus mirabilis* and *Pseudomonas aeruginosa* (Table 3 and figure 5).

Because of the electrostatic force that draws bacteria to the HA's surface, where the calcium and phosphate ions present in hydroxyapatite and the cell membrane of bacteria directly interact, the nanohydroxyapatite (HA) containing plant extract exhibits potent antibacterial activity[16].

The results of this investigation support the theory that radicals possessed antibacterial qualities. HA exhibits antibacterial activity against a range of microbes, according to other investigations. Several causes could account for this feature, the most significant being the release of plant extract and the dissolution of HA. The plant extract interacts with the negatively charged microbial membrane through electrostatic attractions, preventing the microbial growth[1].

Moreover, the -SH groups of microbial enzymes may interact with plant-mediated HA ions to block them. Additionally, microbes can absorb plant extract and have their DNA damaged. Our results demonstrated that Gram negative bacteria were more successfully suppressed by HA than Gram positive bacteria. This is explained by the fact that negatively charged gram negative cell membranes and positively charged Ca^{2+} ions are attracted to each other electrostatically, making it easier for Ca^{2+} and PO_4^{3-} ions to connect to the membrane[12].

Table 3
Antimicrobial activity of developed nanohydroxyapatite from *Terminalia arjuna* bark shows maximum zone of inhibition against both Gram positive and gram negative bacteria

S.N.	Test Pathogen	Zone of Inhibition (in mm)				
		Standard (Streptomycin)	Solvent (Hexane)	Terminalia arjuna bark extract	Nano Hydroxyapatite - Control	Nano Hydroxyapatite - Sample
1	*Staphylococcus aureus*	20	Nil	14	20	22
2	*Bacillus subtilis*	22	Nil	16	20	22
3	*E. coli*	20	Nil	17	18	20
4	*Klebsiella pneumoniae*	18	Nil	14	16	18
5	*Pseudomonas aeruginosa*	16	Nil	16	14	18
6	*Proteus mirabilis*	16	9	15	16	18

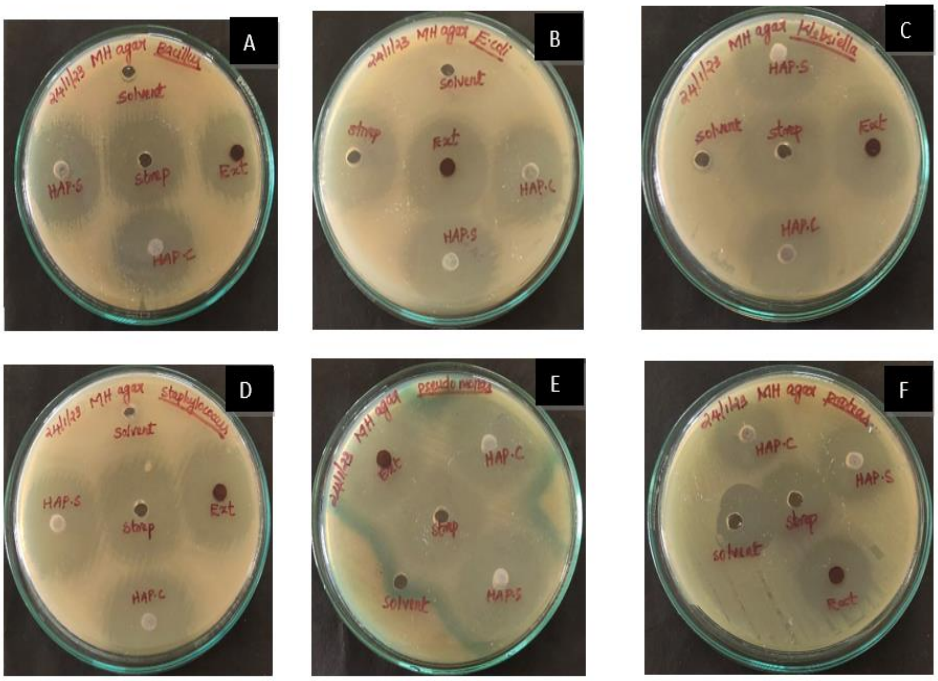

Figure 5: Antimicrobial activity of developed nanohydroxyapatite from *Terminalia arjuna* bark shows maximum zone of inhibition against both Gram positive and gram negative bacteria such as A-*Bacillus subtilis*, B-*Escherichia coli*, C-*Klebsiella pneumoniae*, D-*Staphylococcus aureus*, E-*Pseudomonas aeruginosa* and F-*Proteus mirabilis*. Results are represented as mean ± standard deviation (n=3).

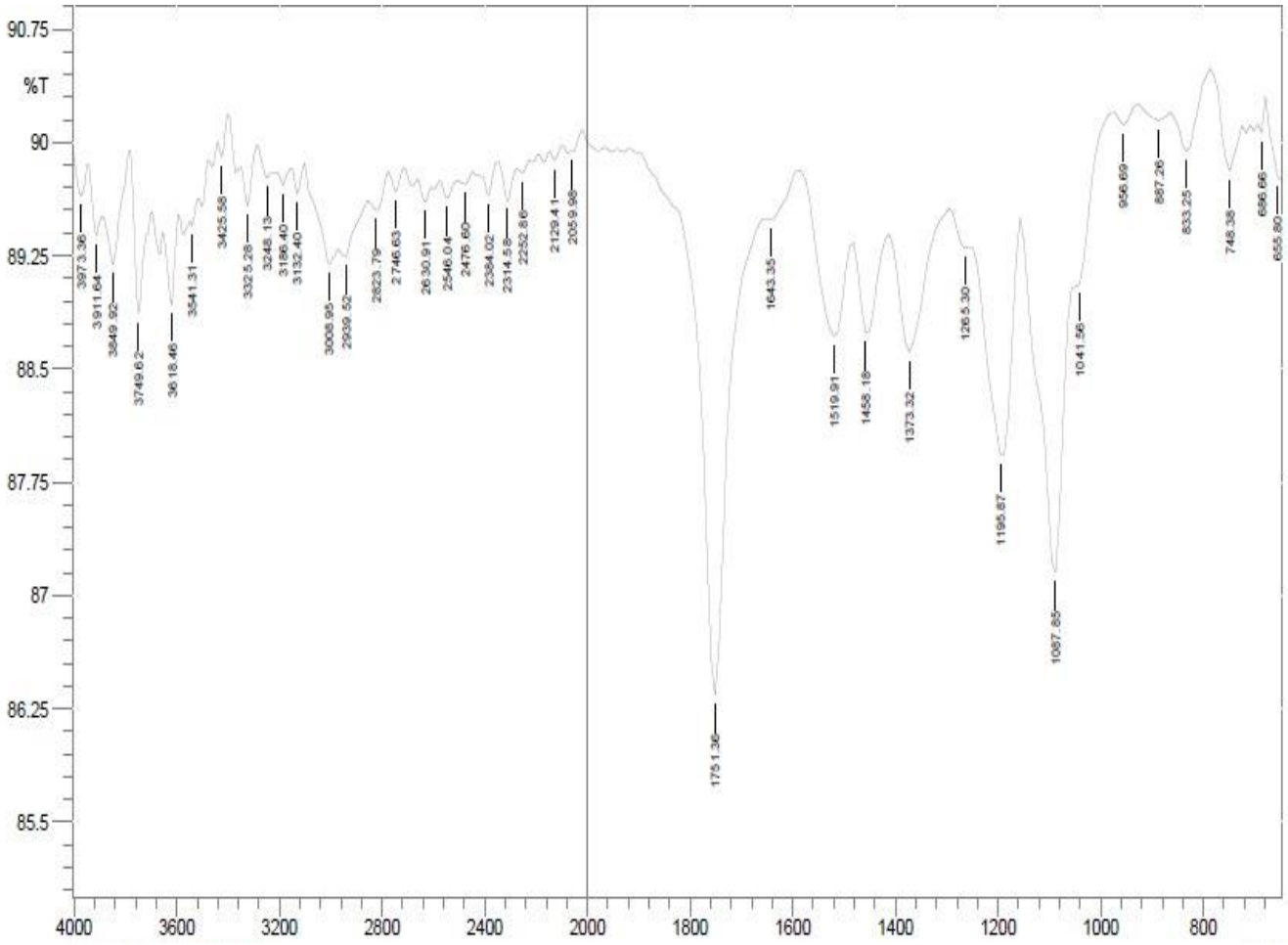

Figure 6: FTIR analysis of developed nanofibrous scaffold which shows the presence of functional groups corresponding to hydroxyapatite and poly-ß-hydroxy butyrate

Electrospinning of developed nanohydroxyapatite using the bark extract of *Terminalia arjuna*: The hydroxyapatite nanoparticle developed from bark extract of *Terminalia arjuna* and PHB (4:2) was dissolved in chloroform and dimethyl formamide (7:3) as an electro spinning solution under magnetic stirrer and stored in a room temperature. Similarly, dichloro methane and dimethyl formamide were used as a solvent with poly caprolactone and developed hydroxyapatite served as an electro spinning solution[38]. The developed electro spinning solution from *Terminalia arjuna* bark extract hydroxyapatite nanoparticle with poly-β-hydroxy butyrate was electro spinned for the duration of 4 hours with flow rate 2500 µl/hr and finally the fibers were collected on a aluminium foil. The fibers were deposited as a nanofibrous mat/scaffold.

Likewise, in order to create the intended scaffold, chitosan and polycaprolactone were electrospun at a distance of 13 cm from the capillaries and for five hours at a voltage of 17 kV. Using polycaprolactone and hydroxyapatite dissolved in methanol and chloroform at a distance of 0.7 mm, 30 kV voltage supply was used to create the nanofibrous scaffold, which was then electrospun[5].

Characterization of developed nanofibrous scaffold Thickness (ASTM D 1777-96): The thickness of *Terminalia arjuna* nanohydroxyapatite with Poly-ß-hydroxybutyrate nanofibrous scaffold was determined as 0.12 mm. In a similar manner, the thickness of hydroxyapatite nanofibrous scaffold with poly caprolactone was determined as 0.11 mm[16].

Tensile Strength (Zwick/Roell): The tensile strength which comprises of the mean breaking strength and mean breaking elongation of the nanofibrous scaffold was developed from *T.arjuna*, along with the strain percent. Mean Breaking Strength Fmax was calculated as 1.43 N. Mean Breaking Elongation dL at Fmax was calculated as 22.9 %. Comparing the *T. arjuna* nanofibrous scaffold to other microfibrous or hybrid scaffolds made of polycaprolactone and hydroxyapatite respectively revealed that the former has greater tensile strength and flexibility[17].

Wetting ability by water contact angle: The wetting ability of the developed nanofibrous scaffold from *T. arjuna* was determined and tabulated in table 4. With 105.30 degrees on the right side and 105.13 degrees on the left, the developed nanofibrous scaffold from *T. arjuna* has an average contact angle of 105.22 degrees. Similarly, hydroxyapatite synthesized with plant extracts exhibited better wetting ability than chemically synthesized routes[22].

Fourier Transform Infrared Spectroscopy analysis of the developed nanofibrous scaffold: The biomolecules and functional groups present in the developed nanofibrous scaffold from *Terminalia arjuna* with poly-β-hydroxy butyrate were analyzed by FTIR. Figure 6 represents the presence of numerous peaks indicating the presence of several compounds in the developed nanofibrous scaffold. 3541.31 cm^{-1} and 3325.28 cm^{-1} were predominant strong peaks that represent the existence of alcoholic functional group. The presence of poly ester 1265.31 cm^{-1} is the most important which confirms the presence of PHB. The carbonate and phosphate groups, which make up the majority of the most important compounds found in hydroxyapatite nanoparticles, are represented by the peaks at 1458.18 cm^{-1} and 887.26 cm^{-1} respectively.

Because the other peaks serve as template agents and precursors for the production of hydroxyapatite nanoparticles, they indicate the presence of secondary metabolites of the extract from *Terminalia arjuna*. The outcome demonstrated that the creation of a nanofibrous scaffold required the integration of nano hydroxyapatite with PHB biopolymer.

Similarly, the FTIR analysis of hydroxyapatite with poly caprolactone nanofibrous scaffold has the presence of prominent peaks which corresponds to the presence of carbonate, phosphate and alcoholic functional groups[24].

Scanning Electron Microscopy analysis of the developed nanofibrous scaffold: The SEM images represent the topology of the electro spunned nano fibers. The SEM micrographs represent the fibers of created nanofibrous scaffolds with diameters ranging from 0.5 to 5 µm. Figure 7 represented the SEM analysis of developed nanofibrous scaffold which has interconnected non-woven fibers. The final nanofibrous mat-like morphology of the hydroxyapatite chitosan composites of nanofibrous scaffold produced a wider distribution of fiber diameters[36].

Bioactivity of developed nanofibrous scaffold: Bioactivity of nanofibrous scaffold was evaluated by the apatite formation on the surface in a simulated body fluid with ion concentration similar to human blood plasma. The Scanning electron microscopy was performed after incubation of scaffold for 7 days at 37˚C in SBF. The SEM images represent the apatite formation present in the nano fibers. The simulated body fluid was prepared according to the Kokubo's protocol.

The result reveals the presence of apatite formation after incubation and hence the developed nanofibrous scaffold has bioactivity. Results obtained from figure 8 represented the apatite formation in SEM analysis to determine the bioactivity of the nanofibrous scaffold. Similar results reported the presence of apatite formation of developed scaffold after immersing in simulated body fluid[17].

***In vitro* cytotoxicity determination of the developed *Terminalia arjuna* nano fibrous scaffold:** A concentration-dependent decrease in cell viability was shown by the cytotoxicity evaluation. The lowest sample concentration (6.25 µg/ml) had the highest percentage viability (96.58 %) indicating a negligible cytotoxic effect, 91. 29 % at 12. 5

µg/ml, 86. 22 % at 25 µg/ml 81. 27 % at 50 µg/ml and 75. 79 % at the highest tested concentration of 100 µg/ml showed a steady decline in cell viability as the sample concentration increased. The toxicity analysis of the developed nanofibrous scaffold in the MG-63 cell line is shown in figure 9 with the inverted phase contrast tissue culture microscopic images (Olympus CKX41 with Optika Pro5 CCD camera) of *in vitro* cytotoxicity evaluation of developed *Terminalia arjuna* nano hydroxyapatite in MG-63 cell line.

Table 4
Water contact angle of the developed nanofibrous scaffold

S.N.	Contact Angle	Degree
1	Right side in degree	105.30
2	Left side in degree	105.13
3	Average contact angle degree	105.22

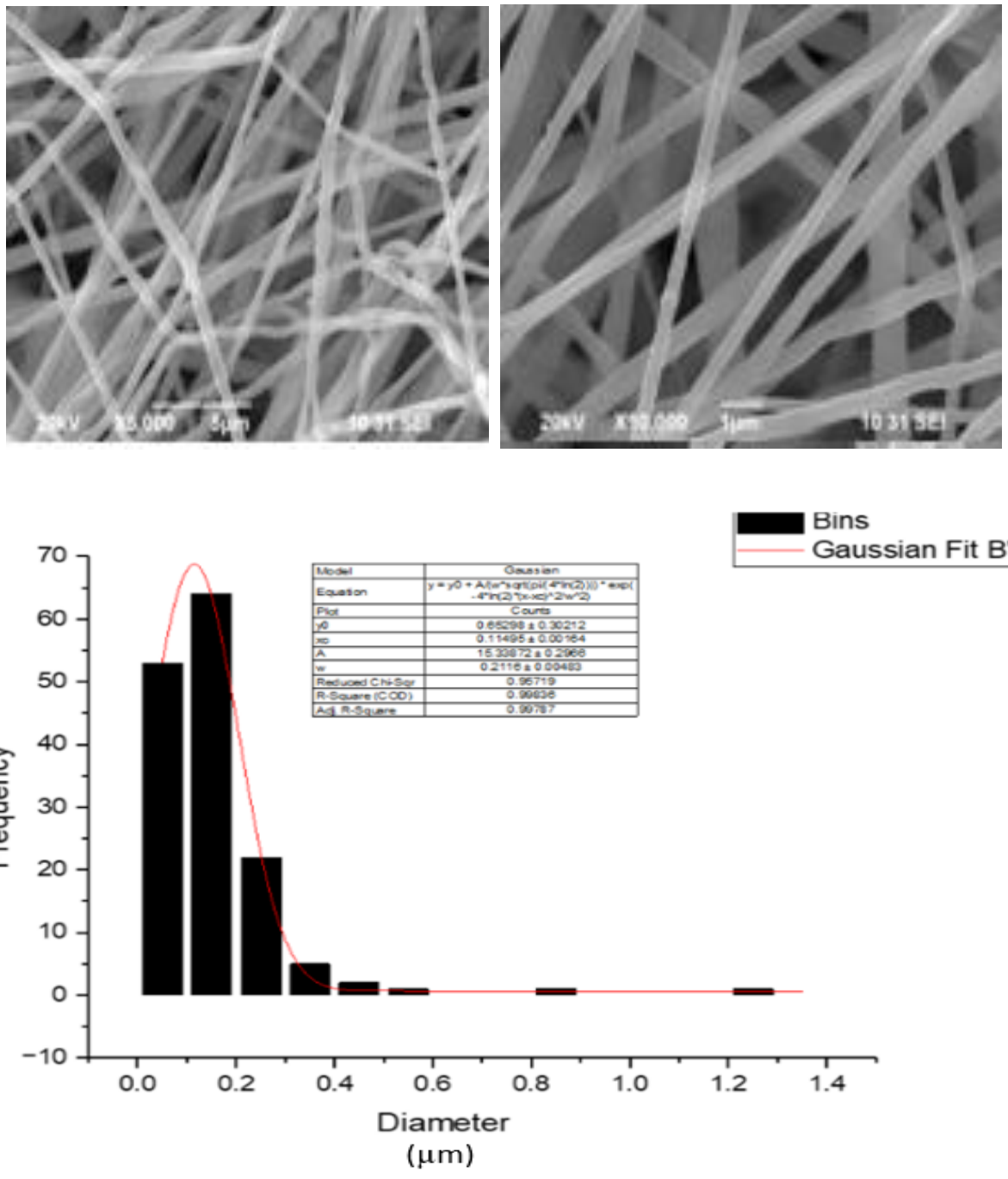

Figure 7: SEM Analysis with particle size distribution of Electrospun nanofibrous scaffold from *Terminalia arjuna* nano fibrous scaffold. A- Electrospun SEM micrographs, B- Particle size distribution graph

As the sample concentration raises, these findings point to a progressive cytotoxic response. The data suggests that the sample may be used in targeted therapeutic applications and the LC50 value is 219.648 µg/ml which was calculated using ED50 Plus V1.0 software. In contrast to the control group, a study examining the effects of Origanum extract (OE) and Rosmarinus extract (RE) on MG-63 cells revealed significant antiproliferative effects at concentrations of 500 µg/mL and 700 µg/mL respectively[38]. Likewise, tomentosin a naturally occurring sesquiterpene lactone demonstrated a reduction in MG-63 cell viability that was both dose- and time-dependent with an IC_{50} value of roughly 40 µM following a 24-hour treatment period[39].

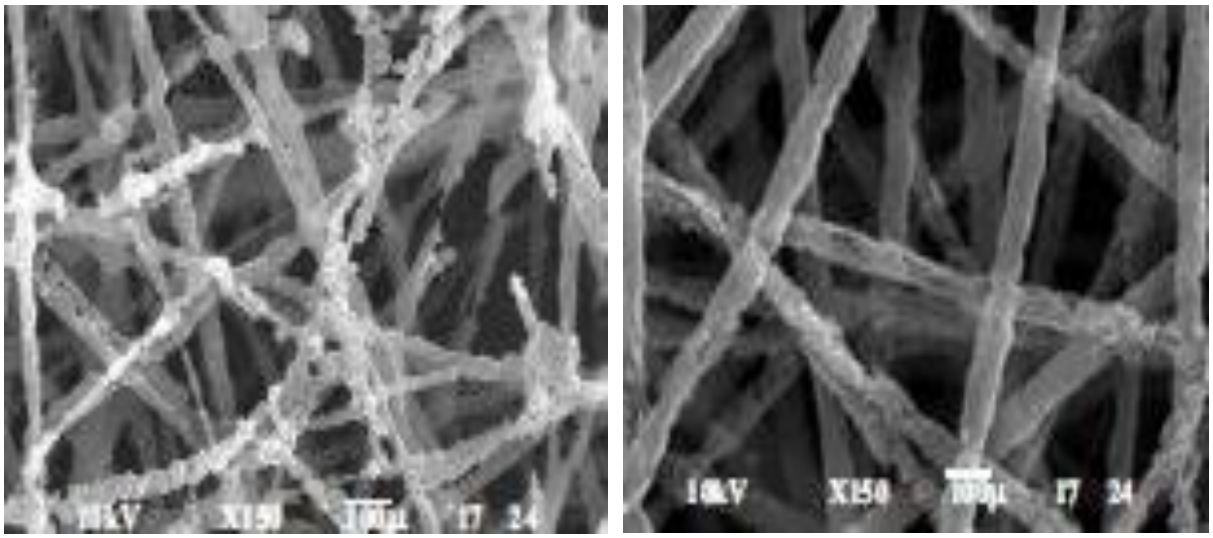

Figure 8: Bioactivity testing in simulated body fluid of Electrospun nanofibrous scaffold which indicates the developed nano fibrous scaffold able to form apatite formation when immersed in SBF, hence the developed nanofibrous scaffold has bioactivity.

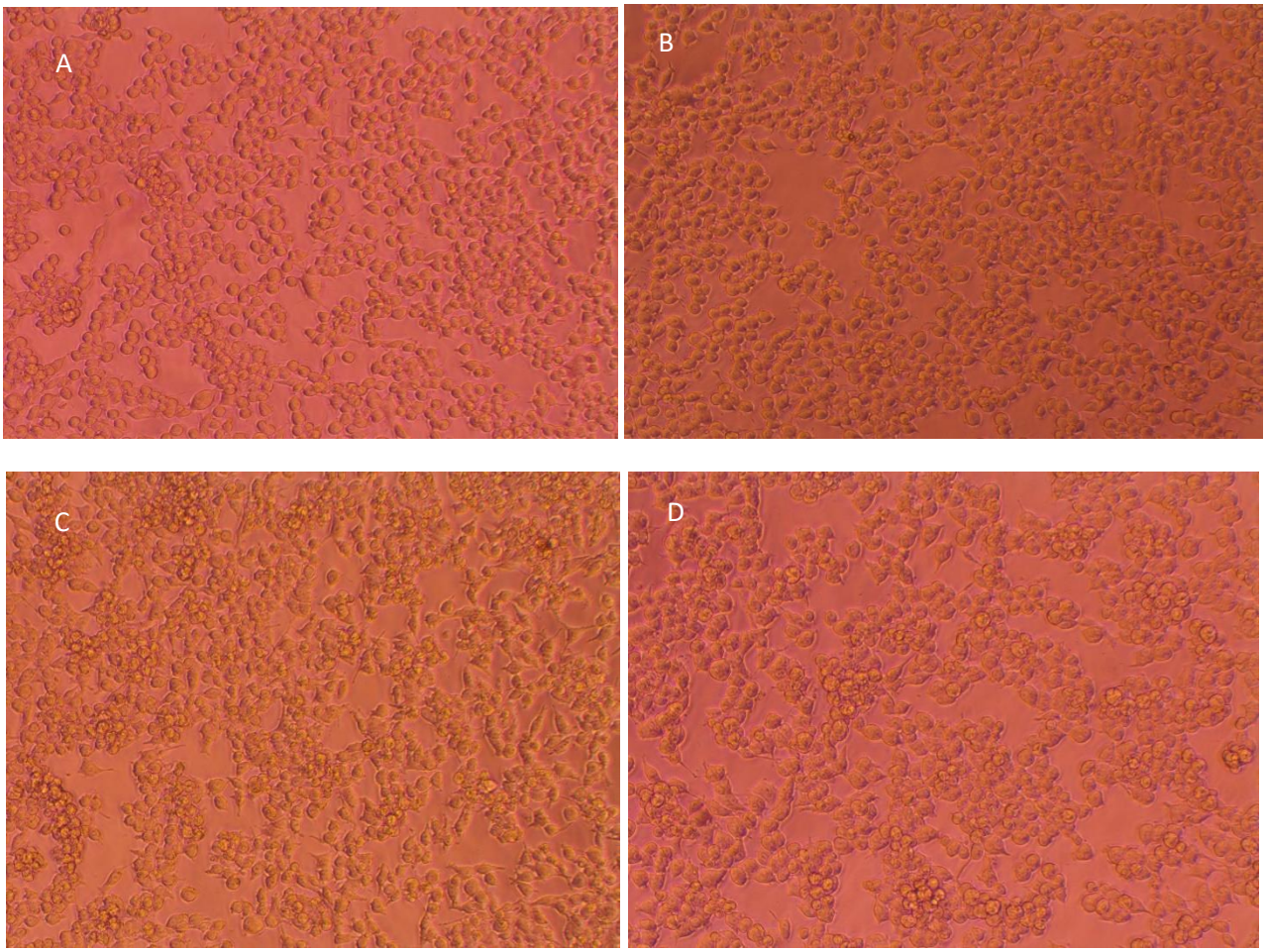

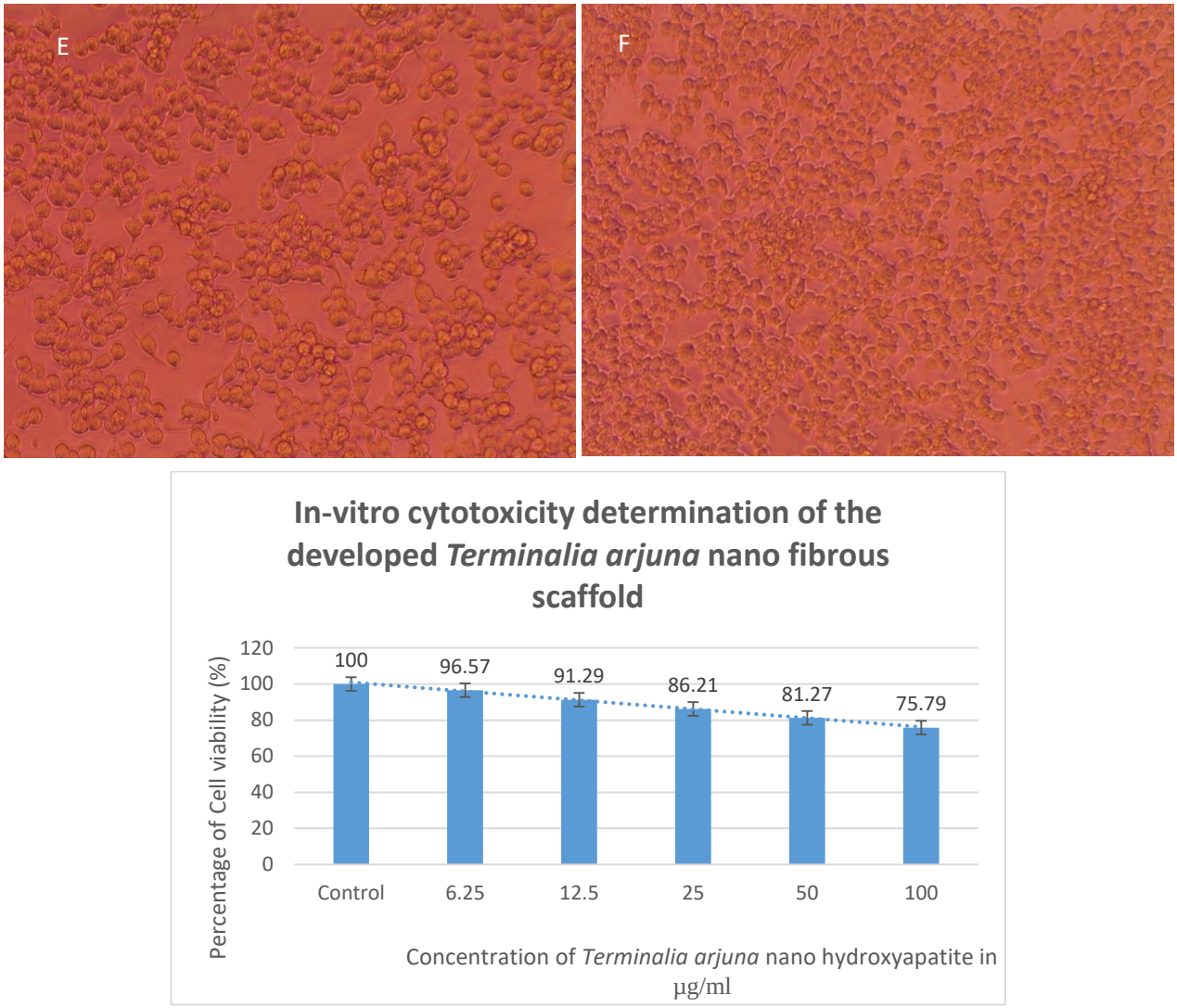

Figure 9: Inverted phase contrast tissue culture microscopic images (Olympus CKX41 with Optika Pro5 CCD camera) of in-vitro cytotoxicity evaluation of developed *Terminalia arjuna* nano hydroxyapatite in MG-63 cell line (Sample) A- 6.25 µg/ml sample concentration, B-12.5 µg/ml sample concentration, C- 25 µg/ml sample concentration, D- 50 µg/ml sample concentration, E- 100 µg/ml sample concentration and F- control (Untreated) and Graphical representation depicting the cytotoxic effect of sample on MG-63 cell line by MTT assay. Along Y axis Percentage viability, Along X axis varied concentration of Sample. All experiments were done in triplicates and results represented as Mean+/- SE. One-way ANOVA and Dunnets test were performed to analyse data. ***p < 0.001 compared to control groups. **p < 0.001 compared to control groups

Osteoprotective effects of the developed *Terminalia arjuna* nano fibrous scaffold: The developed *Terminalia arjuna* nano fibrous scaffold exhibits the osteoprotective effects in the MG-63 cell line after inducing the toxicity. Dexamethasone (5µM) was given to induce toxicity in the cells and were incubated for one hour. The freshly prepared *Terminalia arjuna* nano hydroxyapatite samples concentration from 25 µg/mL, 12.5 µg/mL, 6.25 µg/mL, 3.1 µg/mL and 1.5 µg/mL was added in the five wells which have dexamethasone treated. Untreated control wells were also added and incubated for 24 hours. After incubation, the percentage of cell viability was calculated, in the untreated control group has cell viability 100 %, dexamethasone alone treated has 48.07 %, dexamethasone with the sample treated has cell viability 53.08 % in 1.5 µg/mL, 58.58 % in 3.1 µg/mL, 65.53 % in 6.25 µg/mL, 73.09 % in 12.5 µg/mL and 77.16 % in 25 µg/mL concentration.

The percentage of cell viability of the samples after inducing toxicity was represented in figure 10 with the inverted phase contrast tissue culture microscopic images (Olympus CKX41 with Optika Pro5 CCD camera) of osteoprotective effects of *Terminalia arjuna* nano hydroxyapatite in MG-63 cell line. The present study reveals that the developed *Terminalia arjuna* nano hydroxyapatite exhibits protection in the MG-63 cell line after inducing toxicity because dexamethasone alone treated has only 48.07 % cell viability, while adding the samples the cell viability was increased and thereby confirming that the samples have osteoprotective effects. This effect promotes the bone formation and regeneration by potentially mitigating bone loss associated disease like osteoporosis.

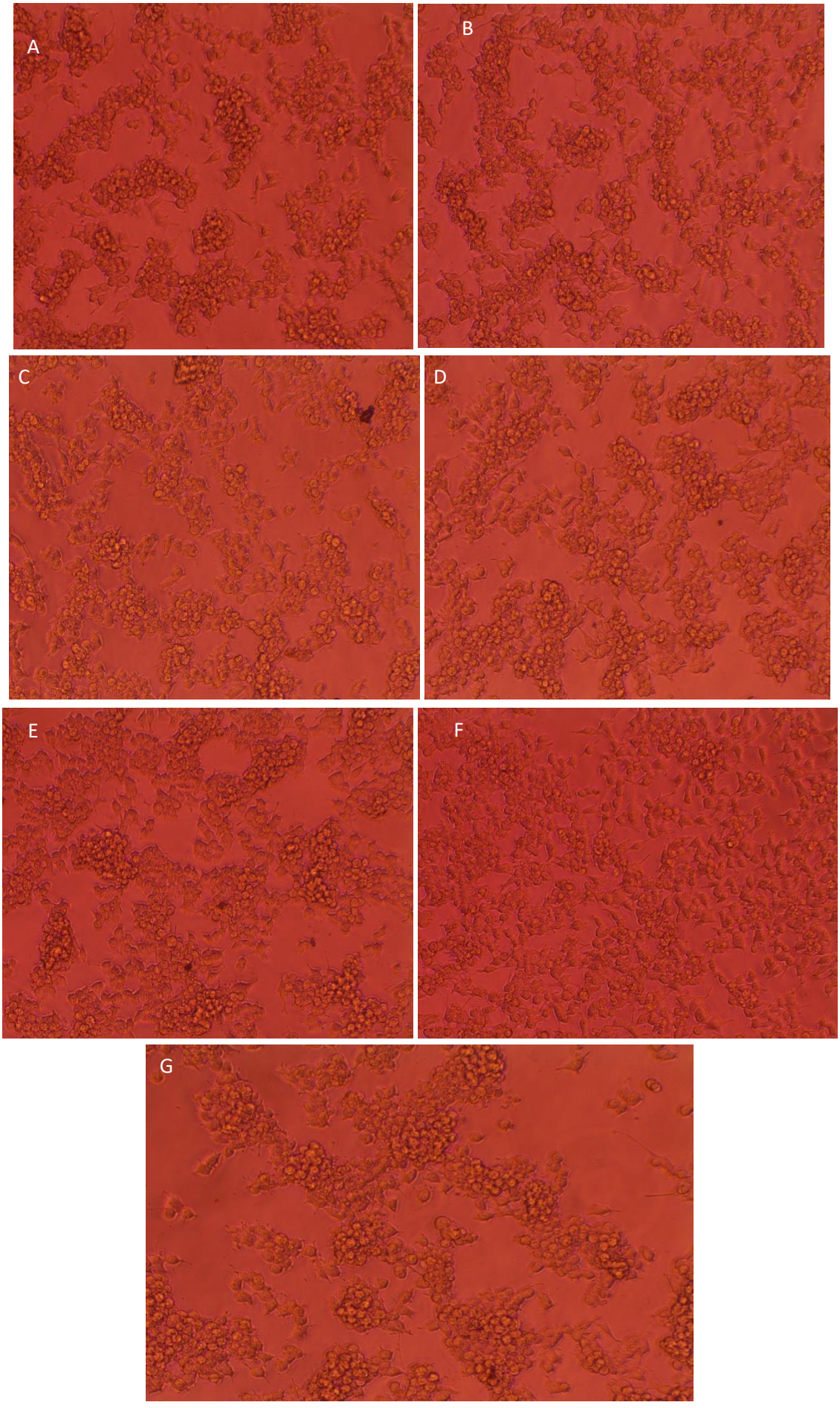
A
B
C
D
E
F
G

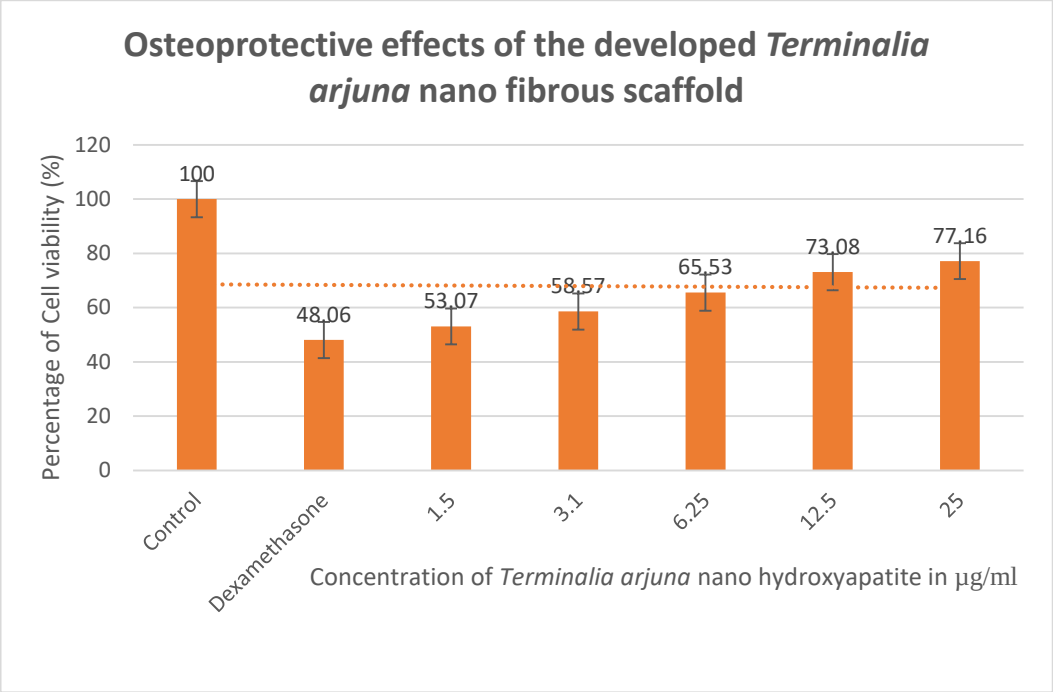

Figure 10: Inverted phase contrast tissue culture microscopic images (Olympus CKX41 with Optika Pro5 CCD camera) of osteoprotective effects of *Terminalia arjuna* nano hydroxyapatite (Sample) in MG-63 cell line A- Dexamethasone with 1.5 µg/ml sample concentration, B- Dexamethasone with 3.1 µg/ml sample concentration, C- Dexamethasone with 6.25 µg/ml sample concentration, D- Dexamethasone with 12.5 µg/ml sample concentration, E- Dexamethasone with 25 µg/ml sample concentration, F- control (Untreated), G- Dexamethasone alone and Graphical representation depicting the osteoprotective effect of sample on MG-63 cell line by MTT assay. Along Y axis Percentage viability, Along X axis varied concentration of sample. All experiments were done in triplicates and results represented as Mean+/- SE. One-way ANOVA and Dunnets test were performed to analyse data. ***p < 0.001 compared to control groups

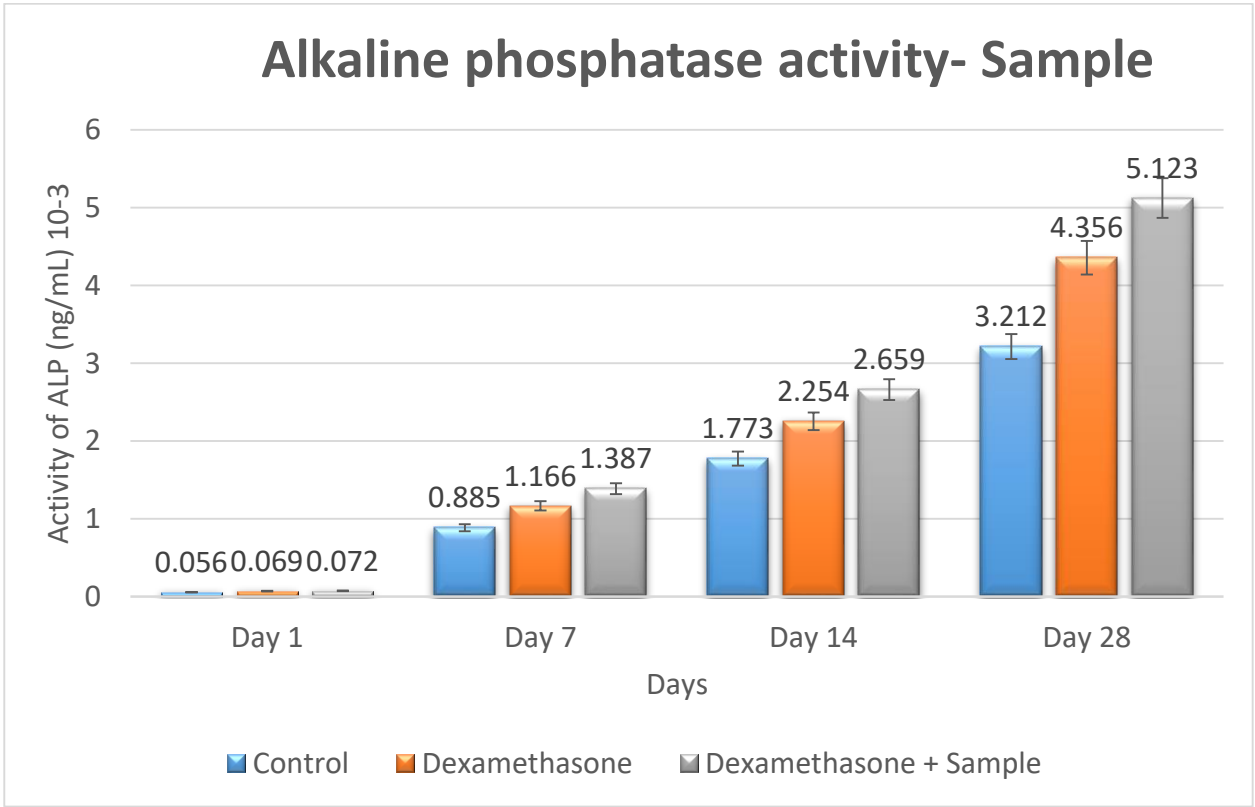

Figure 11: Graphical representation depicting the Activity of Alkaline phosphatase. Along Y axis Activity of ALP (ng/mL) $\times 10^{-3}$, Along X axis sample code with days of incubation

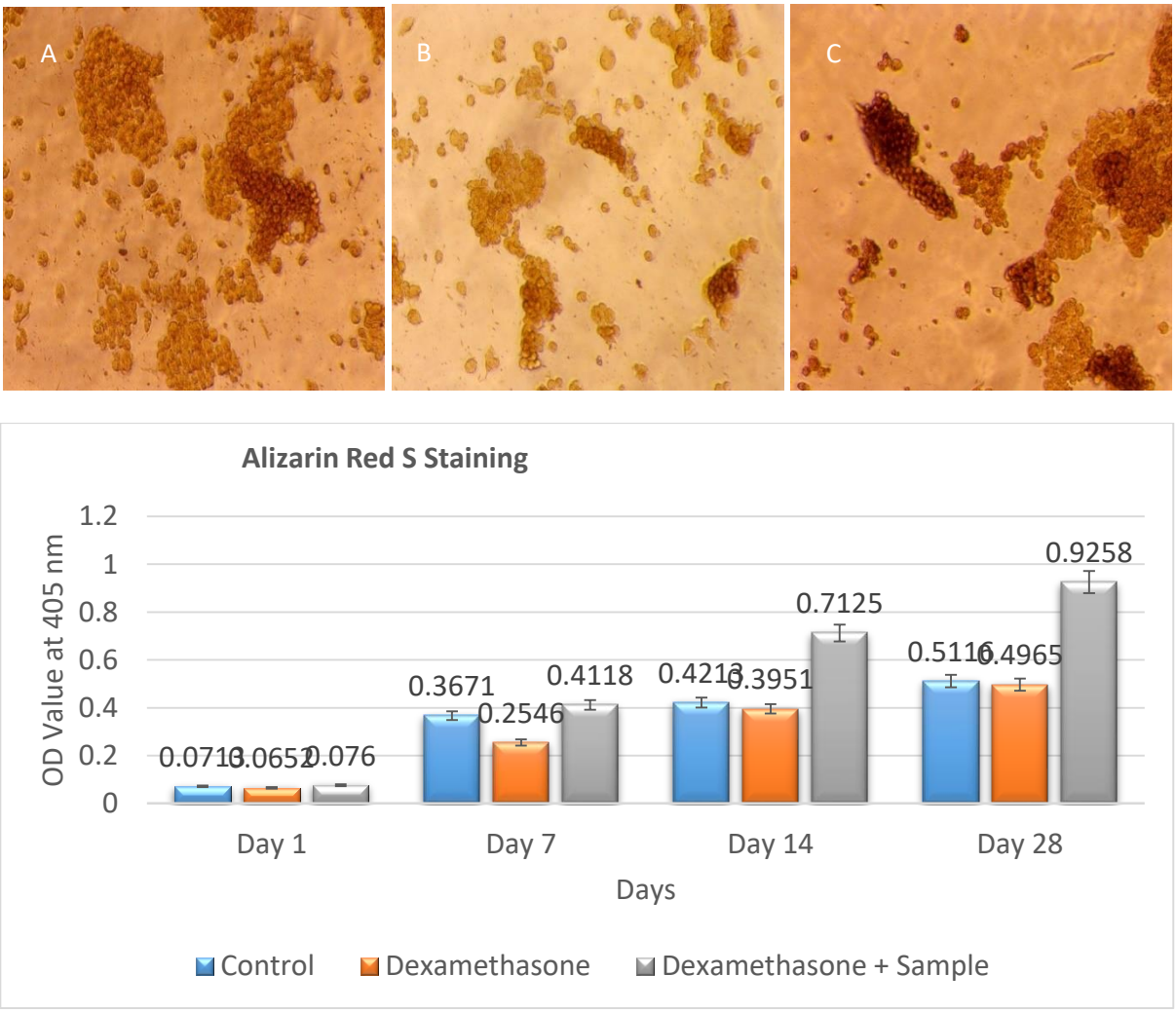

Figure 12: Phase contrast microscopy images of the nodule formation in calcium release assay of the developed *Terminalia arjuna* nano composite by alizarin red staining A- Control (untreated) B- Dexamethasone alone treated and C- *Terminalia arjuna* nano fibrous scaffold with dexamethasone treated with the graphical representation depicting the calcium release assay of the developed *Terminalia arjuna* nano composite

Similarly, the osteoinductive potential of samarium doped hydroxyapatite was evaluated in the MC3T3-E1 preosteoblast cell line. After incubation of 24 hours, the percentage of cell viability was 82 % in 25 µg/mL concentration which indicates the sample promotes osteoinductive property[33]. By interacting with osteoblasts and affecting signaling pathways, nano hydroxyapatite improves osteogenic differentiation and mineralization. In particular it triggers the FAK/AKT pathway which is essential for cell division survival and proliferation. This activation stimulates the production of bone microtissues and raises the expression of osteogenic markers. Further the nano hydroxyapatite materials contribute to the extracellular matrix (ECM) and improve the structural integrity and functionality of newly formed bone tissue by mediating the mineral deposition. In order to facilitate faster bone healing, nano hydroxyapatite acts as a bioactive scaffold that coordinates with cellular mechanisms[17].

Human specific alkaline phosphatase activity of the developed *Terminalia arjuna* nano composite by Sandwich ELISA: *In vitro* human specific ALP of the developed nano composite was done to determine the bone formation activity which is similar to human physiological conditions. Human specific ALP was done in order to avoid cross reactivity with non- human enzymes which provides accurate and relevant results for potential bone regeneration purpose. Figure 11 reveals the levels of ALP activity expressed by the developed *T. arjuna* nano fibrous scaffold at 25 µg concentration on the 1st, 7th, 14th and 28th day. On the 1st day 0.056 ng/ml for control (untreated), 0.069 ng/ml for dexamethasone alone treated and 0.072 ng/ml for sample along with dexamethasone treated, there was no significant difference in ALP activity between the groups.

On the 7th (0.885 ng/ml for control (untreated), 1.166 ng/ml for dexamethasone alone treated and 1.387 ng/ml for sample along with dexamethasone treated), 14th (1.773 ng/ml for control (untreated), 2.254 ng/ml for dexamethasone alone treated and 2.659 ng/ml for sample along with dexamethasone treated) and 28th days (3.212 ng/ml for control (untreated), 4.356 ng/ml for dexamethasone alone

treated and 5.123 ng/ml for sample along with dexamethasone treated) considerable increase in ALP activity was observed more in the developed nano fibrous scaffold along with dexamethasone than the control (untreated) and dexamethasone alone treated cells. This may be due to the influence of *T. arjuna* extract on cell differentiation.

The increase in ALP levels in cells especially under dexamethasone induced stress confirms its ability to stimulate bone forming pathways and counteracts the inhibitory effects of the drug dexamethasone. Increased human ALP activity indicates the bone matrix maturation and mineralization which are very much essential in bone regeneration. ALP activity typically gets decreased due to suppression in osteoblast cells in presence of dexamethasone. Similarly, the concentration of ALP in control and administration of acetaminophen were found to be decreased when compared to *Terminalia arjuna* leaf extract treated[33].

Calcium release assay of the developed *Terminalia arjuna* nano composite by Alizarin Red S staining: ARS staining detects the calcium rich deposits which is a key indicator in late-stage osteoblast differentiation and bone matrix mineralization. Calcium deposition is essential for the mechanical strength of the human bone and this calcium deposition confirms the mature bone formation. Figure 12 reveals the levels of calcium release (mineralization) expressed by the developed *T. arjuna* nano fibrous scaffold at 25 µg concentration on the 1st, 7th, 14th and 28th day. On the 1st day (0.071 for control (untreated), 0.065 for dexamethasone alone treated and 0.076 for sample along with dexamethasone treated), there was no significant difference in mineralization potential between the groups.

On the 7th (0.367 for control (untreated), 0.254 for dexamethasone alone treated and 0.411 for sample along with dexamethasone treated), 14th (0.421 for control (untreated), 0.395 for dexamethasone alone treated and 0.712 for sample along with dexamethasone treated) and 28th days (0.511 for control (untreated), 0.496 for dexamethasone alone treated and 0.925 for sample along with dexamethasone treated) tremendous increase in calcium mineralization was observed more in the developed nano fibrous scaffold along with dexamethasone than the control (untreated) and dexamethasone alone treated cells. Phase contrast microscopy images of the nodule formation in calcium release assay of the developed *Terminalia arjuna* nano composite by alizarin red staining were also reported in the figure 12.

Calcium deposition gets reduced under dexamethasone induced toxicity, hence the restoration or enhancement of calcium deposit through ARS staining by the developed nanocomposite suggested its osteoprotective effect. The significant increase in calcium levels in the developed nano fibrous scaffold may be due to the osteogenic effect of *T. arjuna* bark extract on MG-63 cells. The increased calcium release and osteogenic differentiation of MG-63 cells on collagen and gelatin electron spun scaffolds were reported by Shahatha et al[33].

Conclusion

The nanofibrous scaffolds using biopolymers and plant extracts have been thoroughly investigated for their potential uses in tissue engineering and biomedical applications. They have the capacity to replicate the extracellular matrix with biocompatibility and biodegradability. Through the successful electrospinning of a nanofibrous scaffold containing bark extract of *Terminalia arjuna* with the biopolymer poly-β-hydroxybutyrate, the present study developed a highly porous interconnected fiber network. The developed scaffold has excellent mechanical strength and flexibility which make it appropriate for biomedical applications.

The chemical characterization confirms the presence of important functional groups like carbonate, phosphate, alcohol and polyester bonds which confirmed the successful incorporation of hydroxyapatite nanoparticles made with *Terminalia arjuna* bark extract. Strong diffraction peaks that corresponded to a hexagonal phase in XRD analysis further confirmed the crystalline structure of hydroxyapatite which was compared to standard JCPDS data. The topological analysis by Scanning electron microscope reveals that the developed nano hydroxyapatite were homogeneous nanorod-like shape that closely resembles with nanocrystalline structures found in human bone and that on electrospinning produced uniform distribution of particles.

Strong antibacterial activity was also exhibited by the scaffold against common wound causing pathogens like *S. aureus, E. coli, B. subtilis, Pseudomonas aeruginosa, Proteus mirabilis* and *Klebsiella pneumoniae*. The electrostatic interaction between the positively charged calcium ions from hydroxyapatite and the negatively charged bacterial membranes exhibited significant inhibition of bacterial growth which is important for biomedical application.

Furthermore, the developed scaffold exhibited significant apatite formation when immersed in simulated body fluid confirming its bioactivity potential for bone regeneration. The cytotoxicity test validated the biocompatibility confirming its potential use in biomedical settings. To ascertain the developed scaffold potential as a bone-regenerative therapeutic agent against chemically induced bone loss, osteoprotective effects were investigated. The dexamethasone causes osteoblast cells to undergo apoptosis which lowers bone formation and mimics the symptoms of osteoporosis. The confirmation of osteoprotection was evaluated by human specific ALP activity and calcium release assay by Alizarin red S staining.

Determining the osteoprotective effect using the created

nano composite verifies the viability, proliferation and differentiation of osteoblast cells in the presence of dexamethasone. Hence the present study shows that the developed scaffold serves as a shield for osteoblast bone-forming cells from toxicity. Overall, the nanofibrous scaffold made from *Terminalia arjuna* exhibits remarkable qualities that make it ideal for biomedical applications. In future, the scaffold may also be investigated for drug delivery systems and bone tissue engineering with additional study and improvement broadening its application in tissue engineering and regenerative medicine.

References

1. Abraham A., Kumar S.M., Krishna D. and Sri S.M., Development of nanohydroxyapatite membrane using *Momordica charantia* and study of its biodegradability for medical application, *Biomass Convers. Biorefin.*, **14**, 32289–32301 **(2024)**

2. Al-Harrasi A., Bhatia S., Aldawsari M.F. and Behl T., Plant profile, phytochemistry and ethnopharmacological uses of *Terminalia bellirica*, *Terminalia chebula* and *Terminalia arjuna*, Recent Adv. Nat. Prod. Sci., CRC Press, **4**, 143–172 **(2022)**

3. Alorku K., Manoj M. and Yuan A., A plant-mediated synthesis of nanostructured hydroxyapatite for biomedical applications: a review, *RSC Adv.*, **10**, 40923–40939 **(2020)**

4. Anitha A., Menon D., Sivanarayanan T., Koyakutty M., Mohan C.C., Nair S.V. and Nair M.B., Bioinspired composite matrix containing hydroxyapatite-silica core-shell nanorods for bone tissue engineering, *ACS Appl. Mater. Interfaces*, **9**, 26707–26718 **(2017)**

5. Avila J.D., Stenberg K., Bose S. and Bandyopadhyay A., Hydroxyapatite reinforced Ti6Al4V composites for load-bearing implants, *Acta Biomater.*, **123**, 379–392 **(2021)**

6. Balas M., Badea M.A., Ciobanu S.C., Piciu F., Iconaru S.L., Dinischiotu A. and Predoi D., Biocompatibility and osteogenic activity of samarium doped hydroxyapatite biomimetic nanoceramics for bone regeneration, *Biomimetics*, **9**, 309 **(2024)**

7. Barbanente A., Palazzo B., Esposti L.D., Adamiano A., Iafisco M., Ditaranto N., Migoni D., Gervaso F., Nadar R. and Ivanchenko P., Selenium-doped hydroxyapatite nanoparticles for potential application in bone tumor therapy, *J. Inorg. Biochem.*, **215**, 111334 **(2021)**

8. Bee S.L. and Hamid Z.A.A., Hydroxyapatite derived from food industry bio-wastes: syntheses, properties and its potential multifunctional applications, *Ceram. Int.*, **46**, 17149–17175 **(2020)**

9. Garai C., Hasan S.N., Barai A.C., Ghorai S., Panja S.K. and Bag B.G., Green synthesis of *Terminalia arjuna*-conjugated palladium nanoparticles (TA-PdNPs) and its catalytic applications, *J. Nanostruct. Chem.*, **8**, 465–472 **(2018)**

10. Hokmabad V.R., Davaran S., Aghazadeh M., Alizadeh E., Salehi R. and Ramazani A., A comparison of the effects of silica and hydroxyapatite nanoparticles on poly(ε-caprolactone)-poly(ethylene glycol)-poly(ε-caprolactone)/chitosan nanofibrous scaffolds for bone tissue engineering, *Tissue Eng. Regen. Med.*, **15**, 735–750 **(2018)**

11. Ibraheem S.A., Audu E.A., Jaafar M., Adudu J.A., Barminas J.T., Ochigbo V., Igunnu A. and Malomo S.O., Novel pectin from *Parkia biglobosa* pulp mediated green route synthesis of hydroxyapatite nanoparticles, *Surf. Interfaces*, **17**, 100360 **(2019)**

12. Irshad N., Hameed H., Mumtaz M., Aslam Z., Batool A. and Sohail I., *Terminalia arjuna* restores the levels of alkaline phosphatase and aspartate aminotransferase of acetaminophen intoxicated mice, *Adv. Life Sci.*, **10(1)**, 104–108 **(2023)**

13. Kalaiselvi V., Mathammal R., Vijayakumar S. and Vaseeharan B., Microwave assisted green synthesis of hydroxyapatite nanorods using *Moringa oleifera* flower extract and its antimicrobial applications, *Int. J. Vet. Sci. Med.*, **6**, 286–295 **(2018)**

14. Kostadinova A., Benkova D., Staneva G., Hazarosova R., Vitkova V., Yordanova V. and El-Sayed K., Chitosan hybrid nanomaterials: a study on interaction with biomimetic membranes, *Int. J. Biol. Macromol.*, **276**, 133983 **(2024)**

15. Krithiga G., Hemalatha T., Deepachitra R., Ghosh K. and Sastry T.P., Study on osteopotential activity of *Terminalia arjuna* bark extract incorporated bone substitute, *Bull. Mater. Sci.*, **37**, 1331–1338 **(2014)**

16. Li L., Li H., Wang Q., Xue Y., Dai Y., Dong Y. and Lyu F., Hydroxyapatite nanoparticles promote the development of bone microtissues for accelerated bone regeneration by activating the FAK/Akt pathway, *ACS Biomater. Sci. Eng.*, **10**, 4463-4479 **(2024)**

17. Lowe B., Hardy J.G. and Walsh L.J., Optimizing nanohydroxyapatite nanocomposites for bone tissue engineering, *ACS Omega*, **5**, 1–9 **(2020)**

18. Mohapatra S., Leelavathi L., Rajeshkumar S., Sri Sakthi D. and Jayashri P., Assessment of cytotoxicity, anti-inflammatory and antioxidant activity of zinc oxide nanoparticles synthesised using clove and cinnamon formulation – an *in-vitro* study, *J. Evol. Med. Dent. Sci.*, **9**, 1859–1864 **(2020)**

19. Moodley J.S., Krishna S.B.N. and Pillay K., Sershen and Govender P., Green synthesis of silver nanoparticles from *Moringa oleifera* leaf extracts and its antimicrobial potential, *Adv. Nat. Sci. Nanosci. Nanotechnol.*, **9**, 015011 **(2018)**

20. Mounika S. and Ramakrishnan P., Synthesis and comparison of chemical challenges using FTIR spectroscopy for copper substituted hydroxyapatite, E3S Web Conf., **477**, 00083 **(2024)**

21. Mushtaq A., Zhao R., Luo D., Dempsey E., Wang X., Iqbal M.Z. and Kong X., Magnetic hydroxyapatite nanocomposites: the advances from synthesis to biomedical applications, *Mater. Des.*, **197**, 109269 **(2021)**

22. Noviyanti A.R., Akbar N., Deawati Y., Ernawati E.E., Malik Y.T., Fauzia R.P. and Risdiana, A novel hydrothermal synthesis of nanohydroxyapatite from eggshell-calcium-oxide precursors, *Heliyon*, **6**, e03655 **(2020)**

23. Obada D.O., Osseni S.A., Sina H., Salami K.A., Oyedeji A.N., Dodoo-Arhin D. and Fasanya O.O., Fabrication of novel kaolin-reinforced hydroxyapatite scaffolds with robust compressive strengths for bone regeneration, *Appl. Clay Sci.*, **215**, 106298 **(2021)**

24. Oliver-Urrutia C., Kashimbetova A., Slámečka K., Casas-Luna M., Matula J., Koledova Z.S. and Montufar E.B., Porous titanium/hydroxyapatite interpenetrating phase composites with optimal mechanical and biological properties for personalized bone repair, *Biomater. Adv.*, **166**, 214079 **(2025)**

25. Orooji Y., Mortazavi-Derazkola S., Ghoreishi S.M., Amiri M. and Salavati-Niasari M., Mesoporous Fe_3O_4@SiO_2-hydroxyapatite nanocomposite: green sonochemical synthesis using strawberry fruit extract as a capping agent, characterization and their application in sulfasalazine delivery and cytotoxicity, *J. Hazard Mater.*, **400**, 123140 **(2020)**

26. Padrao T., Coelho C.C., Costa P., Alegrete N., Monteiro F.J. and Sousa S.R., Combining local antibiotic delivery with heparinized nanohydroxyapatite/collagen bone substitute: a novel strategy for osteomyelitis treatment, *Mater. Sci. Eng. C*, **119**, 111329 **(2021)**

27. Raj S., Singh H., Trivedi R. and Soni V., Biogenic synthesis of AgNPs employing *Terminalia arjuna* leaf extract and its efficacy towards catalytic degradation of organic dyes, *Sci. Rep.*, **10(1)**, 9616 **(2020)**

28. Reena G., Kiran G. and Kamlesh P., Effect of anabolic steroid in accelerating healing process of experimentally fractured tibia of rats and compare its fracture healing property with *Terminalia arjuna*, *Int. J. Curr. Microbiol. App. Sci.*, **5(5)**, 788–795 **(2016)**

29. Roozbahani M., Kharaziha M. and Emadi R., Fabrication and characterization of laponite-calcium phosphate based cement for filling bone defects, *Mater. Today Proc.*, **5**, 15754–15760 **(2018)**

30. Ryabenkova Y., Pinnock A., Quadros P., Goodchild R., Möbus G., Crawford A., Hatton P. and Miller C., The relationship between particle morphology and rheological properties in injectable nano-hydroxyapatite bone graft substitutes, *Mater. Sci. Eng. C*, **75**, 1083–1090 **(2017)**

31. Said M.M., Rehan M., El-Sheikh S.M., Zahran M.K., Abdel-Aziz M.S., Bechelany M. and Barhoum A., Multifunctional hydroxyapatite/silver nanoparticles/cotton gauze for antimicrobial and biomedical applications, *Nanomaterials*, **11**, 429 **(2021)**

32. Sathiskumar S., Vanaraj S., Sabarinathan D., Bharath S., Sivarasan G., Arulmani S., Preethi K. and Ponnusamy V.K., Green synthesis of biocompatible nanostructured hydroxyapatite from *Cirrhinus mrigala* fish scale—a biowaste to biomaterial, *Ceram. Int.*, **45**, 7804–7810 **(2019)**

33. Shahatha A.A., Taha S.H. and Mohammed M.A., Preparation and characterization of hydroxyapatite, titania-porous bioceramic via polymeric sponge method, *Biochem. Cell Arch.*, **20**, 1415–1419 **(2020)**

34. Sossa P.A.F., Giraldo B.S., Garcia B.C.G., Parra E.R. and Arango P.J.A., Comparative study between natural and synthetic hydroxyapatite: structural, morphological and bioactivity properties, *Rev. Mater.*, **23,** e-12217, DOI:10.1590/s1517-707620180004.0551 **(2018)**

35. Suba Sri M., Subhashini M., Kalpana Devi M., Jayakala Devi and Usha R., Green synthesis of nano hydroxyapatite using *Calotropis procera* and *Wrightia tinctoria* plant latex serum extract for biomedical application, *Biomass Convers. Biorefin.*, **14**, 19393–19407 **(2024)**

36. Subramanian R., Sathish S., Murugan P., Mohamed Musthafa A. and Elango M., Effect of piperine on size, shape and morphology of hydroxyapatite nanoparticles synthesized by the chemical precipitation method, *J. King Saud Univ. Sci.*, **31**, 667–673 **(2019)**

37. Torabinejad B., Mohammadi-Rovshandeh J., Davachi S.M. and Zamanian A., Synthesis and characterization of nanocomposite scaffolds based on triblock copolymer of L-lactide, ε-caprolactone and nano-hydroxyapatite for bone tissue engineering, *Mater. Sci. Eng. C*, **42**, 199–210 **(2014)**

38. Tsai S.W., Liou H.M., Lin C.J., Kuo K.L., Hung Y.S., Weng R.C. and Hsu F.Y., MG63 Osteoblast-Like Cells Exhibit Different Behavior when Grown on Electrospun Collagen Matrix versus Electrospun Gelatin Matrix, *PLoS One*, **7**, e31200 **(2012)**

39. Yang C., Huan Z., Wang X., Wu C. and Chang J., 3D printed Fe scaffolds with HA nanocoating for bone regeneration, *ACS Biomater. Sci. Eng.*, **4(2)**, 608–616 **(2018)**

40. Zastulka A., Clichici S., Tomoaia-Cotisel M., Mocanu A., Roman C., Olteanu C.D. and Mocan T., Recent trends in hydroxyapatite supplementation for osteoregenerative purposes, *Materials*, **16**, 1303 **(2023)**

41. Zhang L. and Webster T.J., Nanotechnology and nanomaterials: promises for improved tissue regeneration, *Nano Today*, **4**, 66–80 **(2009)**.

(Received 19th June 2025, accepted 23rd July 2025)